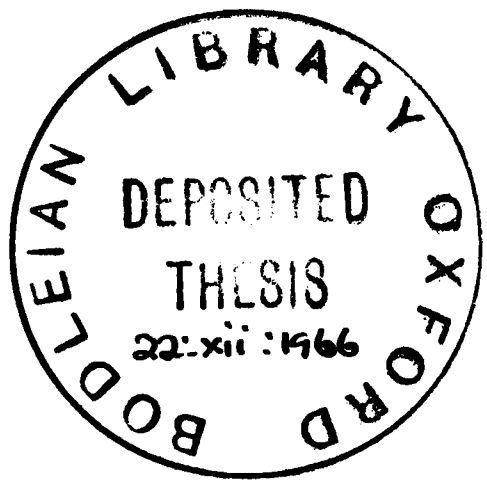
PROBLEMS IN THE QUANTUM THEORY OF MANY-PARTICLE SYSTEMS

A Thesis
submitted for the Degree of Doctor of Philosophy
at the University of Oxford

by

William W. Lewis



July 19, 1966

ABSTRACT

A finite temperature perturbation theory for the Heiserberg model of ferromagnetism is presented. A modified Wick's theorem proved for $S=\frac{1}{2}$ and finite temperatures allows the terms in the expansion for the temperature dependent Green's function to be expressed by linked Feynman-like diagrams. The diagrams differ from the usual boson and fermion diagrams in the appearance of time (temperature) dependent dotted lines between propagators reflecting the effect of spin statistics. For temperatures such that $\frac{T}{T_c}$ is finite, the diagrams for the irreducible self-energies are classified with respect to a high density parameter $\frac{1}{Z}$ where Z is the number of spins interacting with a given spin. The results of molecular field theory are found in first order. The next two orders in the self-energy graphs yield at low T spin wave theory and Dyson's results in Born approximation respectively. The high density classification is also verified directly at low T, and in an appendix, higher order graphs are found to yield the expressions for the lifetimes of the excitations of the system given by Tahir-Kheli and ter Haar. The magnetization expression obtained from the graphs of the first three orders yields a Curie point since the first order graphs are renormalized to include in their internal lines all graphs of all other orders considered. The Curie point found is that of molecular field theory. The expressions for the magnetization at low temperatures and near the Curie point are then used as a guide in approximating the magnetization from graphs of the first three orders at all temperatures. This

approximate expression is calculated as a function of the temperature using a long range potential, and the curve is compared to the experimental results for the magnetization of Cu K_2 Cl_4.$2H_2O$, a spin ½ ferromagnetic insulator with next nearest neighbor interactions. The results from the random phase approximation of Tyablikov and Englert are also compared with the experimental results, and it is seen that both curves fit within the experimental errors of the points up to $\frac{T}{T_c} \sim .6$, but both fall below the experimental points as the Curie temperature is approached. The difference between the two theoretical curves is negligible.

CONTENTS

		Page No.
INTRODUCTION		1
CHAPTER I –	Thermodynamic Perturbation Theory	8
	A. S-Matrix Expansion for the Green's Function	9
	B. Wick's Theorem	12
	C. Diagrammatic Representation	18
	D. Linked Cluster Theorem	24
	E. Definition of Irreducible Self-Energy; Dyson's Equation; Renormalization Technique	26
CHAPTER II –	$\frac{1}{Z}$ Ordering of Diagrams	28
	A. Appearance of $\frac{1}{Z}$ in the Expansion	29
	B. Classification of Graphs	32
CHAPTER III –	Low Temperatures	36
	A. Contributions from Graphs Through Order $\frac{1}{Z^2}$	37
	B. Direct Check on $\frac{1}{Z}$ Ordering	46
CHAPTER IV –	Curie Temperature	49
	A. Curie Point from Graphs Through Order $\frac{1}{Z}$	50
	B. Curie Point from Graphs Through Order $\frac{1}{Z^2}$	51
CHAPTER V –	Approximation of $\frac{1}{Z^2}$ Contributions to Magnetization at all Temperatures; Comparison to Experiment	59
	A. Approximation of $\frac{1}{Z^2}$ Contributions to Magnetization at all Temperatures	60
	B. Experimental Results	63
	C. Calculation of Approximate Curve and RPA Curve for Magnetization with Long Range Potential; Comparison with Experiment	65

		Page No.
CONCLUSION		73
APPENDIX A	Calculation of G^{o}; Molecular Field Theory	75
APPENDIX B	Summation of Order $\frac{1}{Z}$ Graphs	81
APPENDIX C	Evaluation of Integral in RPA Calculation	83
APPENDIX D	Evaluation of Integral in Approximate Formula Calculation	85
APPENDIX E	Lifetimes of Excitations at Low Temperatures	87

Introduction

The Heisenberg model for a ferromagnet is a system of interacting spins with each spin located at a definite point in a lattice. Thus, the Heisenberg model should approximate a ferromagnetic crystal having the properties of an insulator. The discovery of a number of ferromagnetic insulators in recent years has provided an excellent opportunity for comparing experimental results with the predictions of statistical theories of the ideal Heisenberg ferromagnet. In this thesis, an approximate solution, valid at all temperatures, is obtained for the thermodynamic behaviour of the ideal Heisenberg ferromagnet, and a calculation is then done to compare this theoretical prediction with the experimental results for one of the ferromagnetic insulators.

The results of molecular field theory give a good first approximation for the thermodynamic behaviour of a ferromagnetic insulator. The magnetization curve predicted decreases monotonically as the temperature increases until a certain critical temperature is reached beyond which the magnetization is zero in zero yield. The most obvious experimental fact that molecular field theory does not predict is that at low temperatures, the magnetization goes to zero as the sum of terms proportional to $T^{3/2}$ (Weiss, 1937, using Fe_3Al) and $T^{5/2}$ (Gossard, Jaccarino and Remeika, 1961, using $CrBr_3$). Molecular field theory predicts that the magnetization goes to zero as $e^{-\frac{1}{T}}$. The correct results are given by linear spin wave theory (Bloch 1930), and hence, attempts to obtain improvements on molecular field theory valid throughout the entire temperature range have all sought to recover linear spin wave theory at low temperatures. Also

Brout (1960,61) shows that for the Ising model, molecular field theory is obtained in the limit of $\frac{1}{Z} \longrightarrow 0$ where Z is the number of spins interacting with a given spin. Thus, it is often suggested that molecular field theory is also recovered in the limit of $\frac{1}{Z} \rightarrow 0$ for the Heisenberg model, and that improvements on the molecular field theory would be obtained by finding the next order terms in a $\frac{1}{Z}$ expansion for the results of the Heisenberg model.

In recent years there have been several attempts to obtain, for all temperatures, an improvement on the molecular field theory solution for the thermodynamic behaviour of the ideal Heisenberg ferromagnet. These attempts may be divided into two groups. The first (Bogolyubov and Tyablikov 1959, Zubarev 1960, Tahir-Kheli and ter Haar 1962, and Callen 1963) employs the equations of motion of the "advanced" and "retarded" Green's functions, and the solution is obtained through a decoupling of the infinite chain of coupled equations appearing. One form of this approximation is referred to as the "random phase approximation" or RPA. The second type of approach (Stinchcombe, Horwitz, Englert, Brout 1963) uses direct temperature dependent perturbation theory to obtain an expansion for the desired operator in terms of the small parameter $\frac{1}{Z}$. The expansion is then terminated at a given order of smallness and the solution obtained. This thesis extends the development of the latter type of approach.

The results of the method using RPA are in good agreement with the observed thermodynamic behaviour of ferromagnets which can be approximated by the Heisenberg model. At low temperatures, linear spin wave theory is

recovered, but as the temperature is increased, a deviation term proportional to T^3 appears in the expression for the magnetization. As the temperature is further increased, the magnetization decreases monotonically until its zero field value is zero for all temperatures beyond a well defined critical temperature. The critical temperature is shown by Englert (1960) to be that of the spherical model of Berlin and Kac (1952).

However, the RPA results do not agree with Dyson's (1956) low temperature expression for the magnetization. Dyson finds the first deviation from linear spin wave theory to be proportional to T^4. Unfortunately, experiments are unable to distinguish between a T^3 and a T^4 term in the low temperature magnetization. Callen (1963) attempts to resolve the discrepancy between the T^3 and the T^4 terms by using a symmetric decoupling procedure in the equations of motion and then normalizing the new energy terms with appropriate factors proportional to $\langle S_z \rangle$ to obtain a Curie point. He now finds at low temperatures a T^4 term in the magnetization instead of a T^3 term for all spins except for spin ½. Although this procedure is ad hoc, it has motivated a computer calculation by Copeland and Gersch (1966) to find the form of Callen's normalizing factor giving the best fit to experimental curves for the magnetization.

Also, it is not known to what parameter of smallness the RPA approximation of replacing the operator S_z by its average value $\langle S_z \rangle$ corresponds. In an attempt to obtain some information about the RPA approximation itself and to extend the high density approach of Brout to the Heisenberg model, Stinchcombe et al. turn to direct temperature

dependent perturbation theory. They develop a formal expansion for a given operator with the Heisenberg Hamiltonian using the quantum mechanical analogue of classical semi-invariants. For $\frac{T}{T_c}$ finite, the terms in the expansion can be classified according to their order with respect to the high density parameter $\frac{1}{Z}$ (Brout 1960,61). The terms in the expansion are also classified with respect to an expansion in powers of the temperature. At low temperatures, the temperature expansion for the magnetization yields Dyson's results in Born approximation, and near the Curie point the first two orders in the high density classification yield molecular field theory in order 1 and spin wave theory in order $\frac{1}{Z}$. To obtain a satisfactory Curie point, a completely renormalized version of the theory analogous to that of Horwitz and Callen (1961) for the Ising model is necessary. Because of the complexity of the renormalization procedure, an approximation on the higher order terms is made, and the resulting expression for the magnetization leads to the same critical temperature as that of molecular field theory. Thus this expression has a Curie point and avoids the difficulty M. Block (1962) finds when she tries to extend Dyson's low temperature expression for the magnetization self-consistently to the Curie point. Her solution becomes double valued as it approaches the Curie point, indicating that the magnetization makes a discontinuous jump to zero at the Curie point. Also, when the expression of Stinchcombe et al. giving the Curie point is extrapolated to low temperatures, a T^3 term in the magnetization expansion is found. Hence, this expression is similar to RPA and gives an indication of the approximation involved in that theory.

The purpose of this thesis is to extend this latter development by defining more precisely the appearance of the parameter of smallness, $\frac{1}{Z}$, and by including all the order $\frac{1}{Z^2}$ terms. The resulting expression for the magnetization is then compared with the experimental results for one of the ferromagnetic insulators. To accomplish this a modified Wick's theorem for finite temperatures and spin ½ is proved. This allows the terms in the perturbation expansion for the temperature dependent "casual" Green's function to be expressed as products of Green's functions of the same type and simple time (temperature) dependent factors giving the sign which reflect the effect of spin statistics. These terms are simpler than the semi-invariants used previously. Also, a more powerful renormalization and summation technique which avoids some of the mathematical complexity of the semi-invariant method is used in the diagrammatic representation. The diagrams obtained differ from the usual boson and fermion Feynman diagrams by the appearance of dotted lines between the propagators representing the time (temperature) dependent factors.

From the solution for this Green's function, it is possible to obtain expressions for the thermodynamic variables of the system. It is shown that when all the $\frac{1}{Z^2}$ terms are included, an expression for the magnetization is obtained which reduces to Dyson's results in Born approximation at low temperatures and which yields the Curie point of molecular field theory. The expressions for the magnetization at low temperatures and at T_c are then used as a guide in approximating the $\frac{1}{Z^2}$ contributions to the magnetization at all temperatures. The resulting magnetization expression is calculated and compared with experimental results for $CuK_2Cl_4.2H_2O$, a spin ½ ferromagnetic insulator.

Other attempts to fit experimental magnetization curves which may be compared to the calculations in this thesis are those of G. Low (1963) using interacting spin wave theory for EuO and EuS, Miedema, van Kempen and Huiskamp (1963) using interacting spin wave theory with nearest neighbor interactions for $CuK_2Cl_4.2H_2O$, Wood and Dalton (1965) using linear spin wave theory with next nearest neighbor interactions included for $CuK_2Cl_4.2H_2O$, and Carleton, Brout and Stinchcombe (1965) using RPA for the antiferromagnet MnF_2.

This thesis is divided into five main sections. In Chapter I, the perturbation expansion for the Green's function is developed, the modified Wick's theorem is proved, the diagrammatic representation is presented, and the expansion is shown to be a linked cluster expansion. Also, the renormalization and summation techniques are introduced. The parameter of smallness $\frac{1}{Z}$ is put into the expansion in Chapter II, and a classification of the graphs according to the $\frac{1}{Z}$ order of the self energies is made for $\frac{T}{T_c}$ finite. Molecular field theory is found in the lowest order 1, and spin wave theory in order $\frac{1}{Z}$. The order $\frac{1}{Z^2}$ graphs are also picked out. In Chapter III a low temperature approximation is made on the graphs of order $\frac{1}{Z^2}$ and the result for the magnetization from graphs through order $\frac{1}{Z^2}$ is seen to be the same as Dyson's in Born approximation. A direct check of the $\frac{1}{Z}$ order of the terms appearing shows that the $\frac{1}{Z}$ ordering is the same as that obtained in Chapter II for $\frac{T}{T_c}$ finite and in agreement with the known low temperature ordering. Also, in an appendix, graphs of higher order in $\frac{1}{Z}$ are found at low temperatures to give expressions for the lifetimes of the excitation energies in agreement with the results of

Tahir-Kheli and ter Haar (1962). The Curie point region is investigated in Chapter IV. The graphs of order $\frac{1}{Z}$ give the molecular field Curie point, but a condition on the potential which is not necessarily true is also found. This difficulty is removed when all the graphs of order $\frac{1}{Z^2}$ are included, and the molecular field theory Curie point is obtained. Finally, in Chapter V the expressions for the magnetization at low T and at the Curie point are used as a guide in approximating the $\frac{1}{Z^2}$ contributions to $\langle S_z \rangle$ at all temperatures. The resulting theoretical magnetization curve for a long range potential is compared with the experimental results for $CuK_2Cl_4 \cdot 2H_2O$, a ferromagnetic insulator with spin ½ and next nearest neighbor interactions. Since this substance has next nearest neighbor interactions, it might be described by the long range potential or high Z approximation used in this thesis. The RPA magnetization curve is also compared with the experimental results. The conclusion is that both theoretical curves fit the experimental points at low temperatures but that both curves fall below the experimental points near the Curie temperature. The difference between the two theoretical curves is seen to be negligible. The method of calculation of both the theoretical curves is also discussed.

CHAPTER I

THERMODYNAMIC PERTURBATION THEORY

In this chapter the formal perturbation theory used in the thesis is presented. The methods of quantum field theory as given by Abrikosov, Gorkov, and Dzyaloshinski (1963) are closely followed. Previous attempts to use the methods of quantum field theory for the Heisenberg model have been made by Dyson (1956) and Mills, Kenan and Korringa (1960). Dyson attacks the problem by transforming from the non-orthogonal spin wave states to the orthogonal harmonic oscillator states and uses these latter states to evaluate his matrix elements. However, the transformation functions are complicated, and he is able to obtain results only under an approximation valid at low temperatures. Mills, Kenan and Korringa do not transform the spin operators and states, but obtain an expansion in which the effects of spin statistics appear directly. This expansion is of the same form as that in this thesis; however, they make an effective field approximation on the Hamiltonian in an attempt to minimize the complications introduced by the spin statistics. Their results are mostly formal.

In section A of this chapter, the temperature dependent Green's function is defined, the Hamiltonian introduced, and the perturbation expansion developed. The terms in the expansion are simplified through a modified Wick's theorem in section B, and a diagrammatic representation for these terms is presented in section C. In section D a linked cluster theorem is proved for the expansion and in section E the re-normalization and summation techniques are introduced.

A. $\mathcal{S}$-Matrix Expansion for the Green's Function

In analogy with the S matrix expansion of quantum field theory, it is possible to develop a perturbation expansion for the temperature dependent Green's function. The operators appearing in this Green's function differ from ordinary Heisenberg operators in that the variable "it" in the exponentials has been replaced by a ficticious variable "τ" ranging from 0 to β (Matsubara 1955).

This Green's function for the spin case is defined as:

$$G(i,j) = - < P \left\{ \tilde{S}_i^+(\tau_i) \, \tilde{S}_j^-(\tau_j) \right\} > \qquad (I1)$$

where i and j designate lattice sites and

$$\tilde{S}_i^+(\tau_i) = e^{H\tau_i} \, S_i^+ \, e^{-H\tau_i} \qquad S_i^+ = S_i^x + i \, S_i^y$$

$$\tilde{S}_j^-(\tau_j) = e^{H\tau_j} \, S_j^- \, e^{-H\tau_j} \qquad S_j^- = S_j^x - i \, S_j^y \; . \qquad (I2)$$

The tilda designates operators in the "Heisenberg" representation. P is the Dyson chronological operator which simply arranges the operators in order of decreasing times from left to right with no sign changes involved. If an S^+ and an S^- operator have the same time, the S^- is always taken on the left since this is the order of the operators in the Hamiltonian to be introduced.

The brackets < > indicate a statistical mechanical average

$$<Q> = \frac{\mathrm{Tr} \left\{ e^{-\beta H} \, Q \right\}}{\mathrm{Tr} \; e^{-\beta H}} \qquad (I3)$$

where H is taken to be the Heisenberg Hamiltonian with an external field B.

$$H = - h \sum_i S_i^z - \tfrac{1}{2} \sum_{i \neq j} v_{ij} \, S_i \cdot S_j$$

$$h = g \, \mu_B \, B, \quad v_{ij} > 0. \tag{I4}$$

For spin ½, $S_i^z = \tfrac{1}{2} - S_i^- \, S_i^+$; hence H may be rewritten

$$H = \left\{ + h + \frac{v(0)}{2} \right\} \sum_i S_i^- \, S_i^+ - \tfrac{1}{2} \sum_{i \neq j} v_{ij} \left[S_i^- \, S_j^+ + S_i^- \, S_i^+ \, S_j^- \, S_j^+ \right] \tag{I5}$$

where $v(0) = \sum_j v_{ij}$ and the constants are dropped. This Hamiltonian may be separated into a soluble part, H_o, and a part which must be treated as a perturbation, H_1.

$$H_o = \left[h + \frac{v(0)}{2} \right] \sum_i S_i^- \, S_i^+$$

$$H_1 = - \tfrac{1}{2} \sum_{i \neq j} v_{ij} \left[S_i^- \, S_j^+ + S_i^- \, S_i^+ \, S_j^- \, S_j^+ \right] . \tag{I6}$$

The first term in H_1 is referred to as the transverse part and the second, as the longitudinal part.

To obtain an expansion for G(i,j) in terms of H_1, the interaction representation is used. An operator $Q(\tau)$ in the interaction representation is defined by

$$Q(\tau) = e^{H_o \tau} \, Q \, e^{-H_o \tau} . \tag{I7}$$

If $\mathcal{S}(\tau)$ is a matrix such that

$$e^{-H\tau} = e^{-H_o\tau}\,\mathcal{S}(\tau), \quad e^{H\tau} = \mathcal{S}^{-1}(\tau)\, e^{H_o\tau} \quad , \tag{I8}$$

then differentiating both sides of the first of these equations with respect to τ and multiplying both sides by $e^{H_o\tau}$ yields

$$\frac{\partial \mathcal{S}(\tau)}{\partial \tau} = - H_1(\tau)\, \mathcal{S}(\tau) \quad . \tag{I9}$$

It should be noted that $H_1(\tau)$ is in the interaction representation. The solution of I9 satisfying the necessary condition $\mathcal{S}(0) = 1$ is

$$\mathcal{S}(\tau) = P \exp \left[- \int_0^\tau H_1(\tau')\, d\tau' \right] \quad . \tag{I10}$$

The P operator appears because the $H_1(\tau)$'s do not commute at different times. By using this $\mathcal{S}$-matrix, it follows, in the familiar way, that G(i,j) may be expressed as:

$$G(i,j) = - \frac{\mathrm{Tr} \left\{ e^{-\beta H_o} P \left[S_i^+(\tau_i)\; S_j^-(\tau_j)\; \mathcal{S}(\beta) \right] \right\}}{\mathrm{Tr} \left\{ e^{-\beta H_o}\, \mathcal{S}(\beta) \right\}}$$

$$= - \frac{< P \left\{ S_i^+(\tau_i)\; S_j^-(\tau_j)\; \mathcal{S} \right\} >_o}{<\mathcal{S}>_o} \tag{I11}$$

where

$$<Q>_o = \frac{\mathrm{Tr}\; e^{-\beta H_o}\, Q}{\mathrm{Tr}\; e^{-\beta H_o}} \quad , \quad \mathcal{S} \equiv \mathcal{S}(\beta) \quad .$$

H_1 enters the expression for G(i,j) only through $\mathcal{S}$. Thus if $\mathcal{S}$ is expanded, an expansion for G(i,j) in terms of H_1 is obtained.

Expanding I10 yields

$$\mathcal{S} = 1 - \int_0^\beta H_1(\tau_1)\, d\tau_1 + \tfrac{1}{2} \int_0^\beta \int_0^\beta d\tau_1\, d\tau_2\, P\left\{H_1(\tau_1)\, H_1(\tau_2)\right\} - \cdots$$

$$= \sum_{n=0}^{\infty} \frac{(-1)^n}{n!} \int_0^\beta \cdots \int_0^\beta d\tau_1 \cdots d\tau_n\, P\left\{ H_1(\tau_1) \cdots H_1(\tau_n)\right\} . \qquad \text{(I12)}$$

Putting this expression into the numerator of I14 yields

$$G(i,j) = - \frac{1}{\langle \mathcal{S} \rangle_o} \sum_{n=1}^{\infty} \frac{(-1)^n}{n!} \int_0^\beta \cdots \int_0^\beta d\tau_1 \cdots d\tau_n$$

$$\times \langle P \left\{ S_i^+(\tau_i)\, S_j^-(\tau_j)\, H_1(\tau_1) \cdots H_1(\tau_n) \right\} \rangle_o . \qquad \text{(I13)}$$

B. Wick's Theorem

For systems of bosons and fermions, it is possible through the use of Wick's theorem to reduce H_o averages of time ordered products of operators to a sum of products of all possible averages of pairs of operators. The latter averages are equal, by definition, to the Green's function with H_o as the Hamiltonian. The proof of a modified Wick's theorem for spin ½ operators is given here, and it is shown how time ordered products of spin operators such as those appearing in equation I13 may be reduced in a manner similar to the boson and fermion cases.

The results of this section and the next are arrived at independently by Wang, Strikman and Callen (to be published) for the case of zero temperature. Also, the results are similar to those of Mills, Kenan and Korringa (1960).

The averages considered are always put into the form $\langle P\{S_1^+(\tau_1)\ S_2^-(\tau_2)\ S_3^+(\tau_3)\ S_4^-(\tau_4)\ldots\}\rangle_0$ by using properties of the P operator to arrange the operators in alternating S^+,S^- order. There must be the same number of S^+ operators as S^- operators or the average vanishes. Because the H_0 density matrix separates into a product of factors each referring to a single site, the H_0 average above factors into a product of H_0 averages with each factor referring to a single site. Since for spin ½ the spin operators referring to a particular site obey anti-commutation relations, it is possible to apply the fermion form of Wick's theorem with suitable modifications.

To prove this modified Wick's theorem, it is necessary to introduce the analogue of the Wick's chronological operator T. The T operator arranges a product of S^+ and S^- operators in order to decreasing time from left to right and multiplies the product by -1 for each interchange of two spin operators of the same site necessary to achieve the chronological order. Again, if an S^+ and an S^- operator have the same time, the S^- is always taken on the left. The P operator appearing previously is replaced by the T operator and factors ξ_{ij} which correct for the sign changes introduced through T.

ξ_{ij} is defined by

$$\xi_{ij} = 1 - 2\,\delta_{ij}\,\theta(\tau_j-\tau_i) \qquad \text{(I14)}$$

where

$$\theta(\tau_j - \tau_i) = \begin{cases} 1 & \text{if } \tau_j > \tau_i \\ 0 & \text{if } \tau_j < \tau_i \end{cases} . \qquad (I15)$$

Thus the P products appearing before may be written in the form:

$$\langle P \left\{ S_1^+(\tau_1)\ S_2^-(\tau_2)\ S_3^+(\tau_3)\ S_4^-(\tau_4)\ \ldots \right\} \rangle_o$$

$$= \langle T \left\{ S_1^+(\tau_1)\ S_2^-(\tau_2)\ S_3^+(\tau_3)\ S_4^-(\tau_4)\ \ldots \right\} \rangle_o \prod_{n \leftarrow m} \xi_{nm} \qquad (I16)$$

with $n \leftarrow m$ meaning n appears to the left of m in the original product. For products ($\prod_{n \leftarrow m} \xi_{nm} = \xi_{12}\, \xi_{13} \ldots \xi_{23}\, \xi_{24}$) in which all the indices refer to the same site, each factor sucn as ξ_{13} is +1 if $\tau_1 > \tau_3$ and -1 if $\tau_1 < \tau_3$, exactly canceling the minus signs introduced by T.

Wick's theorem in its usual fermion form for finite temperatures may be applied to these sub-product averages whose operators refer to one site only. Thus

$$\langle P \left\{ S_i^+(\tau_1)\ S_i^-(\tau_2)\ S_i^+(\tau_3)\ S_i^-(\tau_4) \ldots S_i^+(\tau_{2n-1})\ S_i^-(\tau_{2n}) \right\} \rangle_o$$

$$= \langle T \left\{ S_i^+(\tau_1)\ S_i^-(\tau_2)\ S_i^+(\tau_3)\ S_i^-(\tau_4) \ \ldots\ S_i^+(\tau_{2n-1})\ S_i^-(\tau_{2n}) \right\} \rangle_o \prod_{n \leftarrow m} \xi_{nm}$$

$$= \Big\{ \langle T \left\{ S_i^+(\tau_1)\ S_i^-(\tau_2) \right\} \rangle_o \langle T \left\{ S_i^+(\tau_3)\ S_i^-(\tau_4) \right\} \rangle_o \ldots \langle T \left\{ S_i^+(\tau_{2n-1}) S_i^-(\tau_{2n}) \right\} \rangle_o$$

$$\pm \langle T \left\{ S_i^+(\tau_1)\ S_i^-(\tau_4) \right\} \rangle_o \langle T \left\{ S_i^+(\tau_3)\ S_i^-(\tau_2) \right\} \rangle_o \ldots \langle T \left\{ S_i^+(\tau_{2n-1}) S_i^-(\tau_{2n}) \right\} \rangle_o$$

$$\pm \ldots \Big\} \prod_{n \leftarrow m} \xi_{nm} \qquad (I17)$$

where the last expression is a sum of products of all possible averages of pairs of operators. The sign in front of each term is determined by the numbers of interchanges necessary to rearrange the operators from their order in the large time ordered product to their order in the separate time ordered products.

For the case in which $H=H_o$, the Heisenberg and the interaction representations are the same. Thus, for $H=H_o$ and equal indices, the Green's function defined in equation I1 reduces to

$$g^o(i,i;\ 1,2) = -\ \langle P\ \{S_i^+(\tau_1)\ S_i^-(\tau_2)\}\ \rangle_o. \tag{I18}$$

The factors of the form $\langle T\{S_i^+(\tau_1)\ S_i^-(\tau_2)\}\rangle_o$ appearing in equation I17 differ from these $g^o(i,i)$'s only in the appearance of the T operator in place of the P operator. These factors may be made to coincide exactly with the g^o's by putting the ξ_{nm} factors referring to the two times in each factor with the factor itself. The ξ_{nm} factor just cancels out the sign change introduced by T. Thus

$$\langle T\ \{S_i^+(\tau_1)\ S_i^-(\tau_2)\}\ \rangle_o\ \xi_{12} = \langle P\ \{S_i^+(\tau_1)\ S_i^-(\tau_2)\}\ \rangle_o = -\ g^o(i,i;1,2). \tag{I19}$$

Using this expression, equation I17 may be rewritten

$$\begin{aligned}
&\langle P \left\{S_i^+(\tau_1)\ S_i^-(\tau_2)\ S_i^+(\tau_3)\ S_i^-(\tau_4)\ \ldots\ S_i^+(\tau_{2n-1})\ S_i^-(\tau_{2n})\right\} \rangle_o \\
&= g^o\ (i,i;1,2)\ g^o(i,i;3,4)\ \ldots\ g^o(i,i;2n-1,2n) \prod_{n \leftarrow m} \xi_{nm} \qquad \text{(I20)} \\
&\qquad\qquad\qquad

where $\prod_{n \leftarrow m} \xi_{nm}$ indicates the product $\prod_{n \leftarrow m} \xi_{nm}$ with all the

factors ξ_{nm} referring to times appearing together in an averaged pair or in a g^o deleted. The sign in front of each term is determined by the number of interchanges necessary to rearrange the operators from their order in the large time ordered product to the order of the separate time ordered products and also by the numbers of g^o's in each product. It is noted that since the indices of the ξ functions have the same order as the indices in the original P product, an interchange of two operators which appear together in one of the separate products does not introduce a minus sign.

The g^o's appearing in the above expression may be calculated exactly.

$$g^o(i,j) = - \langle P \{ S_i^+(\tau_i) \; S_j^-(\tau_j) \} \rangle_o$$

$$= \begin{cases} - \dfrac{\mathrm{Tr} \left\{ e^{-\beta H_o} \, e^{H_o(\tau_i - \tau_j)} \, S_i^+ \, e^{-H_o(\tau_i - \tau_j)} \, S_j^- \right\}}{\mathrm{Tr} \, e^{-\beta H_o}} & \tau_i > \tau_j \\ - \dfrac{\mathrm{Tr} \left\{ e^{-\beta H_o} \, e^{-H_o(\tau_i - \tau_j)} \, S_j^- \, e^{H_o(\tau_i - \tau_j)} \, S_i^+ \right\}}{\mathrm{Tr} \, e^{-\beta H_o}} & \tau_i < \tau_j \end{cases} \qquad \text{(I21)}$$

where the property of invariance of the trace under cyclic permutation is used.

$$H_o = \left[h + \frac{v(0)}{2} \right] \sum_i S_i^- \, S_i^+ \, .$$

Thus, from the two identities

$$e^{H_o(\tau_i-\tau_j)}\ S_i^+\ e^{-H_o(\tau_i-\tau_j)} = S_i^+\ e^{-\left[h+\frac{v(0)}{2}\right](\tau_i-\tau_j)} \tag{I22}$$

and

$$e^{-H_o(\tau_i-\tau_j)}\ S_j^-\ e^{+H_o(\tau_i-\tau_j)} = S_j^-\ e^{-\left[h+\frac{v(0)}{2}\right](\tau_i-\tau_j)},$$

it is seen that

$$g^o(i,j) = \left\{\frac{-\,e^{-\left[h+\frac{v(0)}{2}\right](\tau_i-\tau_j)}}{\mathrm{Tr}\ e^{-\beta H_o}}\right\} \times \begin{matrix}\mathrm{Tr}\left\{e^{-\beta H_o}\ S_i^+\ S_j^-\right\} & \tau_i > \tau_j \\ \mathrm{Tr}\left\{e^{-\beta H_o}\ S_j^-\ S_i^+\right\} & \tau_i \leqslant \tau_j\end{matrix}$$

$$= -\,e^{-[h+v(0)](\tau_i-\tau_j)} \begin{cases} \left(1+e^{-\beta\left[h+\frac{v(0)}{2}\right]}\right)^{-1} \delta r_i r_j & \tau_i > \tau_j \\ \left(1+e^{+\beta\left[h+\frac{v(0)}{2}\right]}\right)^{-1} \delta r_i r_j & \tau_i \leqslant \tau_j. \end{cases} \tag{I23}$$

Hence it is possible to generalize equation I20 to include spin operators referring to different sites since the extra pairings involving operators of different sites vanish because of the delta function in g^o. Thus

$$\left\langle P\left\{S_i^+(\tau_i)\ S_j^-(\tau_j)\ S_k^+(\tau_k)\ \ S_\ell^-(\tau_\ell)\ \ldots\right\}\right\rangle_o$$

$$= \pm\ g^o(i,j)\ g^o(k,\ell)\ \ldots \prod_{n\leftarrow m} \xi_{nm} \tag{I24}$$

$$\pm\ g^o(i,\ell)\ g^o(k,j)\ \ldots \prod_{n\leftarrow m} \xi_{nm} \pm \ \ldots\ ,$$

and a Wick's theorem for the spin ½ case at finite temperatures is obtained.

C. Diagrammatic Representation

The various terms of the expansion for G(i,j) in equation I13 can conveniently be represented by a set of diagrams closely resembling Feynman diagrams. The points in the plane are used to represent the set of lattice site, time coordinates on which the spin operators depend. Then the points appearing as arguments for a single function g^o are connected by a solid line, which represents the g^o, and the points i,j appearing as arguments of the exchange integral, v_{ij}, are connected by a wavy line which represents the exchange integral. An arrowhead on the solid line is used to point from the S^+ coordinate to the S^- coordinate. In all diagrams it is understood that the internal time variables are integrated from 0 to β and that the internal site variables are summed over all lattice sites subject to the condition that for a given v_{ij}, $i \neq j$. Without the ξ functions, the diagrams coming from the longitudinal part of H_1 have the same topological form as those for two particle interactions in the boson and fermion cases. The method of representing the ξ functions in both the longitudinal and transverse diagrams is shown after an example of the basic structure is given.

As an illustration of the basic structure of the diagrammtic representation, the first order term in equation I13 is considered.

$$G^{I}(i,j) = -\frac{\frac{1}{2}}{\langle Q^{2}\rangle_{o}} \int_{o}^{\beta} d\tau_{1} \sum_{k\neq\ell} \langle P\{ S_{i}^{+}(\tau_{i})\, S_{j}^{-}(\tau_{j}) \left[S_{k}^{-}(\tau_{1}) S_{\ell}^{+}(\tau_{1}) \right.$$

$$\left. + S_{k}^{-}(\tau_{1})\, S_{k}^{+}(\tau_{1})\, S_{\ell}^{-}(\tau_{1})\, S_{\ell}^{+}(\tau_{1}) \right] v_{k\ell} \}\rangle_{o} \quad \text{(I25)}$$

The basic diagrams for the numerator of equation I25 are given in figures 1a and 1b. Figure 1a presents the longitudinal part and figure 1b, the transverse.

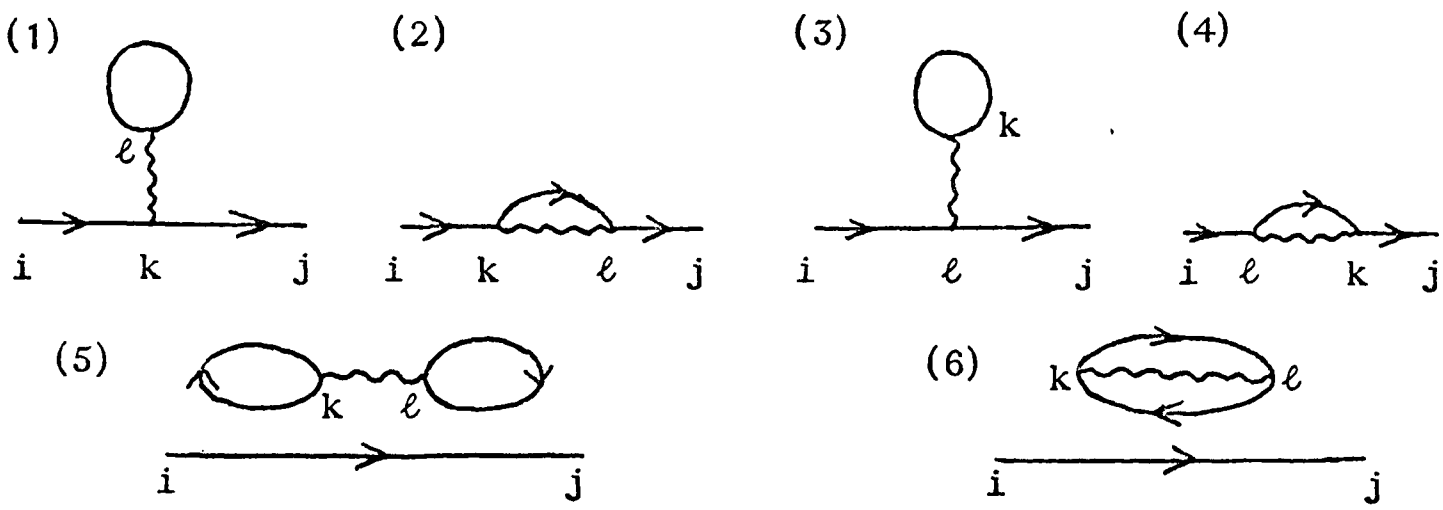


Figure 1a

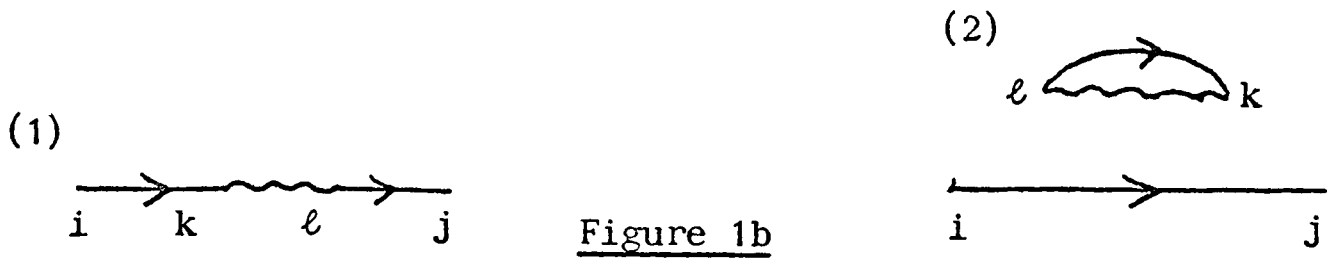


Figure 1b

Graph (1) corresponds to the expression

$$-\tfrac{1}{2} \int_{o}^{\beta} d\tau_{1} \sum_{k\neq\ell}' g^{o}(i,k;\tau_{i}\tau_{1})\, g^{o}(\ell,\ell;\tau_{1},\tau_{1})\, g^{o}(k,j;\tau_{1},\tau_{j})\, v_{k\ell} \,.$$

This expression comes from

$$+\tfrac{1}{2}\int_0^\beta d\tau_1 \sum_{k\neq\ell} \langle P\{S_i^+(\tau_i)\ S_k^-(\tau_1)\}\rangle_0\ \langle P\{S_\ell^+(\tau_1)S_\ell^-(\tau_1)\}\rangle_0 \times$$

$$\langle P\{S_k^+(\tau_1)\ S_j^-(\tau_j)\}\rangle_0\ v_{k\ell}$$

which is one of the terms appearing in the decomposition of equation I25. It snould be noted that the delta function on the site variablesof g^o makes the above graphs zero in many cases.

The ξ functions are introduced into the graphs in the following manner. A dotted line between two solid g^o lines is used to represent the product of the four different ξ functions obtained by taking one of the two ξ function variables from each of the two g^o's. The order of the indices of the ξ function is determined by the order of the operators in the original P product average. The graph in figure 2 represents $g^o(i,j)\ g^o(k,\ell)\ \xi_{jk}\ \xi_{i\ell}\xi_{jk}\xi_{j\ell}$ ... if the original P product average from which this term comes is of the form $\langle P\{S_i^+(\tau_i)S_j^-(\tau_j)S_k^+(\tau_k)\ S_\ell^-(\tau_\ell)\ldots\}\rangle_o$.

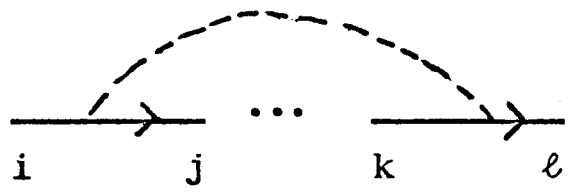


Figure 2

Thus the expansion for G(i,j) indicated by equations I13 and I24 is completely represented by connecting all pairs of solid lines in the basic diagrams by dotted lines. Diagram (2) in figure 1a becomes the graph in figure 3.

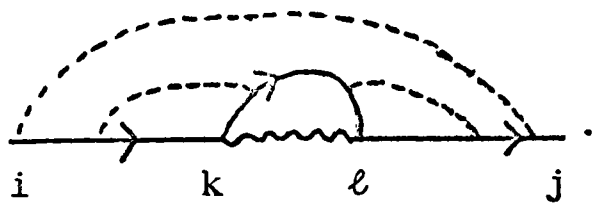


Figure 3

The effect of a dotted line connecting two solid lines such as in figure 2 can be made more explicit. The expression for the graph in fig.2 is zero unless i=j and k=ℓ because of the delta function on g^o, and the dotted line has no effect unless then i=k. With these conditions the P product from which the graph of figure 2 comes is of the form $\langle P\{S_i^+(\tau_1)\ S_i^-(\tau_2)\ S_i^+(\tau_3)\ S_i^-(\tau_4)\ \ldots\}\rangle_o$. If the time variable is taken along the horizontal axis, decreasing from left to right, then the two g^o's coming from the above P product may take many forms, four of which are given in figure 4.

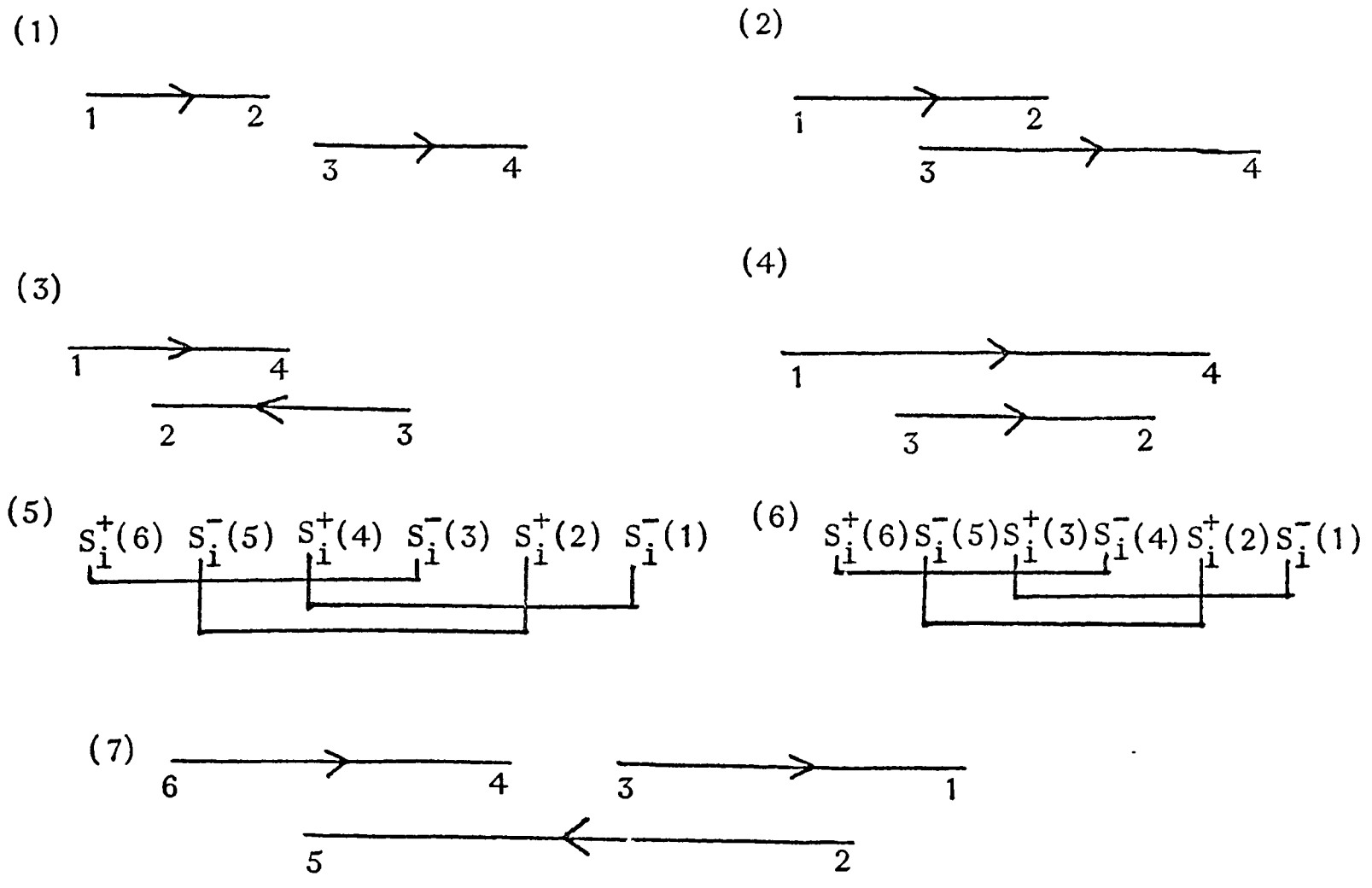


Figure 4

The ξ functions to be associated with diagrams (1) and (2) are the product $\xi_{13}\xi_{14}\xi_{23}\xi_{24}$ and with (3) and (4), $\xi_{12}\xi_{13}\xi_{24}\xi_{34}$. It is seen that the product of ξ functions gives +1 for graphs (1) and (4) and -1 for graphs (2) and (3). The effect of a dotted line between these two g^{o}'s is such as to give a positive sign when the times of the two g^{o}'s are non-overlapping as in graph (1) or completely overlapping as in graph (4) and to give a negative sign when the times are half-overlapping as in graphs (2) and (3).

It is noted that in this case involving only four operators, a change of sign is not introduced by permutations of the operators necessary to achieve the orders of the separate products. However, if there are more operators involved, this sign change may be accounted for by again associating a minus sign with each half-overlap of the times of two Green's functions. If there are three pairs of equal index operators involved and the pairs are those of (5) in figure 4 with the time order 6,5,4,3,2,1, then a minus sign is introduced by the permutation of the operators to form the pairs, but no minus sign is introduced from the ξ functions. The overlapping of the Green's functionsgives this minus sign. If the times of the operators are those shown in (6) with the same order of times as in (5), then there is a minus sign introduced from the permutation of the operators to achieve the pairing and also a minus sign from the ξ_{34} function. It is seen in (7) that there are two half-overlaps of the times of two of the Green's functions giving the necessary plus sign.

This result may be generalized to any numbers of operators. If the pairings of a given set of operators are first displayed as in (5), then

the number of half-overlaps of the contraction lines gives the number of equal index permutations necessary to achieve the pairings not counting permutations over a given pair which gives a plus sign anyway. Then if the operators are not in time order, as (6), rearrangement of the operators to display the overlap of the times of the Green's functions as in (7) accounts for the previous minus sign as well as those coming from the ξ functions associated with the operators. Thus associating a minus sign with each half-overlap of the times of two Green's functions and a plus sign with each non-overlap or complete overlap, accounts for the sign changes introduced by both the permutations of the operators to form the pairs and the ξ functions.

The graphs with dotted lines appearing are treated in the following manner. First the basic graph without the dotted lines is taken, and the integrations over the internal time variables are done freely. Then the effect of one dotted line is taken into account by another diagram in which restrictions on the internal time variables are placed so that the two g^{o}'s connected by the dotted line are half-overlapping during all the integrations. This correction diagram is taken with a factor -2. It is drawn just as the original dotted line graph except with a C written in on the dotted line. The technique is illustrated in figure 5.

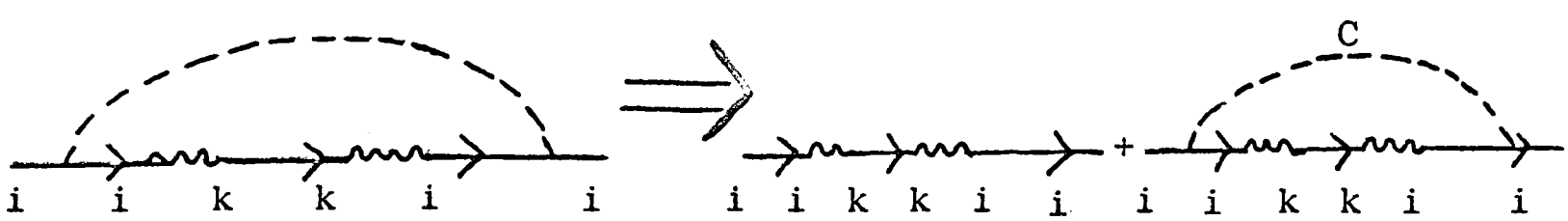


Figure 5

The above procedure is done for each of the dotted lines appearing in the original graph. Then correction graphs to these first correction graphs are added to take into account the effects of two dotted lines giving a minus sign simultaneously. These second correction graphs have two dotted lines with superimposed C's and a factor of +4. This procedure is carried out until the effects of all the dotted lines have been taken into account. The factor associated with a correction graph is $(-2)^C$ where C is the number of correction dotted lines appearing in the graph.

Apart from the factors associated with the correction dotted lines, the sign in front of a graph is determined by the number of g^o's present since the minus signs appearing in the expansion factor $(-1)^n$ are exactly canceled by the minus signs associated with the H_1. Also, each graph carries a factor $(\frac{1}{2})^n$ which comes from the factor $\frac{1}{2}$ in H_1.

D. Linked Cluster Theorem

All the diagrams for the numerator of G(i,j) can be divided into two groups, linked diagrams and unlinked diagrams. A linked diagram is one in which all the points are connected by combinations of solid, wavy, and correction dotted lines to the external points i and j. For example, in figure 6, (1) and (2) are linked but (3) is unlinked.

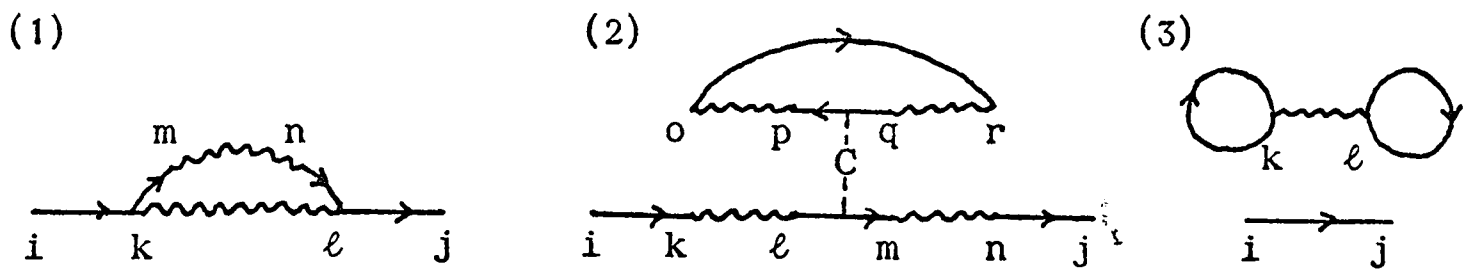


Figure 6

It is shown below how all the unlinked parts which may be associated with a given linked part cancel with the $\langle \mathcal{S} \rangle_0$ in the denominator of G(i,j).

In the expansion of the numerator of G(i,j), a number of diagrams appear which differ only by permutations of the transverse and longitudinal interactions. Such diagrams give identical contributions. Thus it is necessary to consider only one such diagram with the appropriate multiplicity factor. If a diagram of order n has ℓ longitudinal interactions and $t=n-\ell$ transverse interactions, then the multiplicity factor is determined in the following manner. The longitudinal interactions of this particular diagram may be chosen from the product of n H_1's in $\frac{n!}{\ell!(n-\ell)!}$ different ways. But permutations of the longitudinal interactions among themselves give diagrams which correspond to a simple relabeling of the variables of integration and which must give the same contributions. Thus the total multiplicity factor from the longitudinal interactions is $\frac{n!}{(n-\ell)!}$. The site labels of the remaining $n-\ell$ transverse interactions may be distributed in $(n-\ell)!$ ways; hence, the multiplicity factor to be associated with the diagram is n! This n! exactly cancels the expansion factor $\frac{1}{n!}$. The same cancellation occurs in the expansion of $\langle \mathcal{S} \rangle_0$ in the denominator.

Thus it is seen that an unlinked graph consists of a product of independent factors. The expansion of the numerator and denominator differ only in that one factor in the numerator has the external points i and j associated with it. The numerator expansion is just all graphs linked to the external points i and j, multiplied by all graphs unlinked to these graphs. This second factor is just the expansion of $\langle \mathcal{S} \rangle_0$ in the

denominator and cancels with it. Hence, the expansion of G(i,j) reduces to only the linked graphs occurring in the expansion of the numerator.

E. Definition of Irreducible Self-Energy; Dyson's Equation; Renormalization Technique

To obtain useful results from the diagrammatic expansion of G(i,j), it is necessary to sum certain infinite classes of graphs. This is accomplished by using renormalized irreducible self-energies in Dyson's equation.

Any part of a diagram which is joined to the rest of the diagram by two g^0 lines is a self-energy part. An irreducible self-energy part is a self-energy part which cannot be divided into two parts by breaking only one g^0 line. Examples of irreducible self-energies are given in figure 7a.

Every diagram for G of order higher than zero order begins with a g^0 line and some irreducible self-energy part comes next. If these first two parts are cut off from the diagram, the rest of the diagram again begins with a g^0 line followed by an arbitrary number of irreducible self-energy parts joined by g^0's. This later part again corresponds to the exact G function. This result may be represented by the "diagrammatic" equation called Dyson's equation.

$$G = g^0 + g^0 \Sigma G \qquad (I26)$$

where Σ is the sum of all the irreducible self-energies.

It is possible to make the class of graphs associated with each individual self-energy in equation I26 much larger by introducing complete G functions into Σ. These full G functions are represented by heavy lines. Thus the irreducible self-energies in figure 7a become parts of the corresponding renormalized irreducible self-energies in figure 7b. In this renormalization tecnnique, overcounting is avoided by always using the smallest number of G functions possible in the structure of the self-energy.

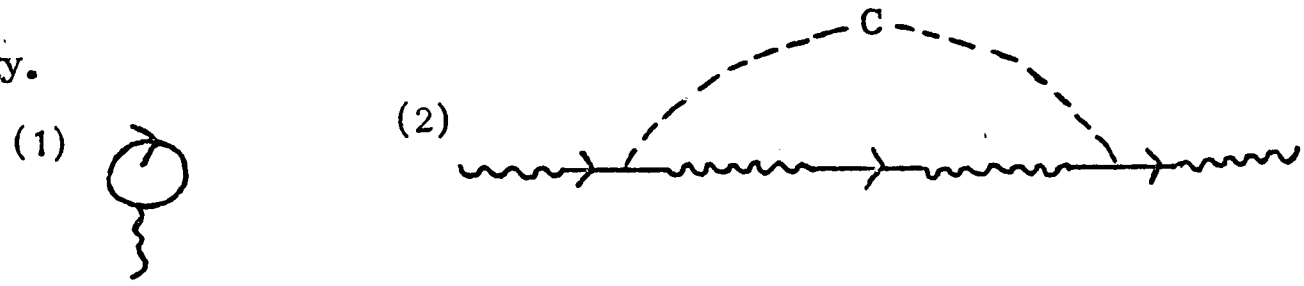


Figure 7a

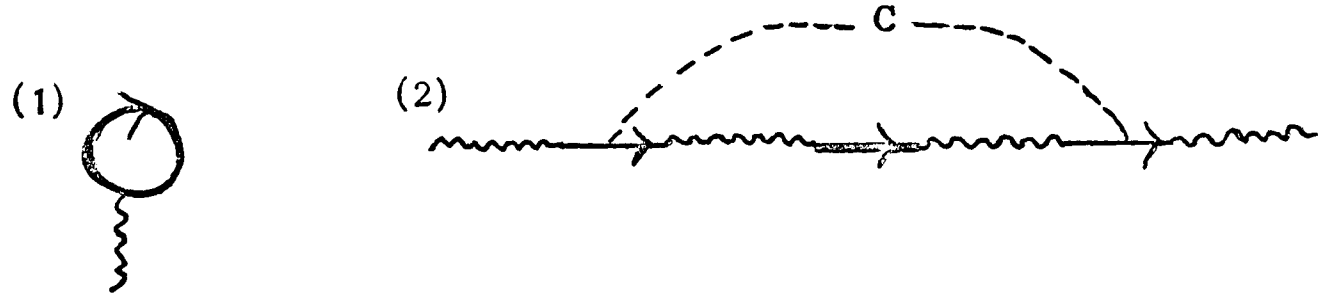


Figure 7b

CHAPTER II

$\frac{1}{Z}$ ORDERING OF DIAGRAMS

At temperatures such that $\frac{T}{T_c}$ is finite, the graphs appearing in the expansion for $G(i,j)$ are classified in this chapter according to their order with respect to a small parameter $\frac{1}{Z}$ with Z being the number of spins interacting with a given spin. For an exchange integral in which only nearest neighbor interactions are important, $\frac{1}{Z}$ is $\frac{1}{6}$ for a simple cubic lattice and $\frac{1}{8}$ for a body centered cubic lattice. However, for longer ranged exchange integrals for which next nearest neighbor interactions are important, $\frac{1}{Z}$ is even smaller.

The parameter $\frac{1}{Z}$ is made to appear in the graphs in the manner of Brout (1960,61), and the argument for the degree of renormalization necessary to make the classification of graphs valid is a variation of the argument given by Horwitz and Callen (1961) for the Ising model. In Section A the parameter $\frac{1}{Z}$ is made explicit in the graphs and in Section B the graphs are classified according to the $\frac{1}{Z}$ order of the irreducible self energies. All the terms through order $\frac{1}{Z^2}$ are picked out. The contribution to G of a given order then is considered to be included if all the irreducible self-energies of that order are included in the self-energy term of Dyson's equation for the summation of graphs. This ordering of the contributions to G is verified at low temperatures in Chapter III by checking directly the $\frac{1}{Z}$ order of the terms appearing.

A. Appearance of $\frac{1}{Z}$ in the Expansion

At β_c and h=0, the parameter $\frac{1}{Z}$ can be made to appear in the graphs in only two ways. First, for each exchange integral $v_{k\ell}$, the sum $\sum_{k\neq\ell}$ produces, in general, Z terms for each allowed k since Z is the number of spins interacting with S_k. The values of k are determined by the values allowed for the site(s) to which the k index is linked through g^0('s). Thus in figure 8, the index k is fixed in the non zero case since it is linked through g^0's to the two operators in the original G which are fixed, and the summation over ℓ produces Z terms. The other way in which $\frac{1}{Z}$ appears is through the factor β which comes from the integration from 0 to β of $d\beta_n$ associated with each interaction term. From molecular field theory, the critical temperature is given for $S=\frac{1}{2}$ by

$$\beta_c \, v(0) = \beta_c \, Z \, \bar{v} = 4$$

where $\bar{v}$ is some average interaction. Thus β_c is proportional to $\frac{1}{Z}$, and at the Curie temperature, a factor $\frac{1}{Z}$ may be associated with each interaction. Using the above prescription, the graph in figure 8 is of order 1 at β_c.

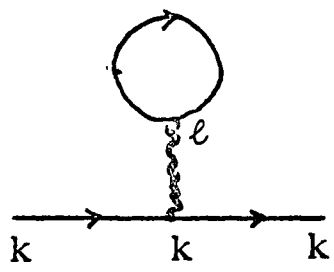


Figure 8

For these ways to be the only ones in which $\frac{1}{Z}$ appears in the graphs, it is necessary to insure that the values of the g^{o}'s themselves at β_c do not change as Z changes. For this condition to be achieved, the g^{o}'s are renormalized to the extent that at the Curie temperature, the averages involved in the g^{o}'s for zero field have the same values as the averages in the full G. The averages in the full G are set such that $R \equiv \langle S_z \rangle = \frac{1}{2} - \langle S_i^- S_i^+ \rangle = 0$, $\bar{n} = \langle S_i^- S_i^+ \rangle = \frac{1}{2}$, and h=0 to define the Curie temperature. A variation in Z is thus reflected only in a variation in β_c and in the number of terms in the summations.

To renormalize the g^{o}'s such that the averages involved in them have the same values at β_c as the averages in G, it is necessary to include in the g^{o}'s all the graphs which yield the averages of molecular field but with a full R appearing indicating that even when other graphs are included, the value of R in each g^{o} is the full R value. This new g^{o}, designated G^{o}, is obtained by summing all graphs generated by the self-energy of the graph in figure 8 and all its correction graphs. The loop in the self-energy is made a full G function indicating that graphs of higher orders which are included at a later time and which contribute to $G(i,i,\tau_1=\tau_2) = -\bar{n}$ are automatically put into the loop. The re-normalization of the loop leads to the appearance of the full R. The details of the calculation of G^{o} are given in Appendix A. The result is

$$G^{o}(i,j) = -e^{-[h+v(0)R](\tau_i-\tau_j)} \begin{cases} [1 + e^{-\beta[h+v(0)R]}]^{-1} & \delta r_i r_j \, \tau_i > \tau_j \\ [1 + e^{+\beta[h+v(0)R]}]^{-1} & \delta r_i r_j \, \tau_i \leq \tau_j \end{cases} . \qquad (II1)$$

At β_c and h=0, $G^0(i,j)$ has the value $-\frac{1}{2}$ for both time orders and does not depend on Z.

It is shown in the next section of this chapter that these molecular field graphs used to renormalize g^0 are the lowest order, order 1, in the $\frac{1}{Z}$ expansion. Thus insertion of G^0's in place of g^0's in a graph of higher order does not change the $\frac{1}{Z}$ order of that graph. Also, the use of the molecular field relation between β_c and Z is strictly justified only for the graphs yielding molecular field theory itself. However, when graphs of higher order are included in Chapter IV, the equation for β_c obtained is that of molecular field theory. Thus the scheme of using the molecular field theory β_c to classify the graphs is consistent even when higher order graphs are included.

It is noted that the graphs may also be classified with respect to their $\frac{1}{Z}$ order at all temperatures such that $\frac{\beta}{\beta_c}$ is finite. In this temperature range the factors of β associated with the interactions are proportional to β_c. Hence the $\frac{1}{Z}$ associated with β_c may also be associated with β, and the same $\frac{1}{Z}$ dependencies are introduced as with β_c. Also, the factors of Z coming from the summations over indices in the graphs are the same as for the β_c case. In addition, for h=0 the G^0's given in equation II1 are independent of Z since for a fixed R, the Z factor introduced by the v(0) in the exponentials is canceled by the $\frac{1}{Z}$ factor associated with β or with $\tau=\tau_i-\tau_j$, which is proportional to β. If τ should be zero, then the first factor automatically has no Z dependence. Thus the classification obtained is the same as that for $\beta=\beta_c$ and h=0.

However, for $h \neq 0$, the G^0's have a $\frac{1}{Z}$ dependence at all temperatures from the βh or $(\tau_i - \tau_j)h$ terms in the exponents. Both of the factors in G^0 may be expanded in this case to give a series in powers of $\frac{1}{Z}$ with the leading term in each series of order 1. Thus, the leading term in G^0 is also of order 1. When the graphs are classified, each G^0 contributes a series in powers of $\frac{1}{Z}$, and each graph is consequently expressed by a series in $\frac{1}{Z}$. However, the order of the graph taken is the lowest order in $\frac{1}{Z}$ appearing, and the lowest order comes from taking the order 1 term from each G^0. The resulting classification is thus exactly that arrived at for $h=0$ where the G^0's are Z independent.

B. Classification of Graphs

In this section, the graphs appearing in the expansion of G in Chapter I are classified according to their order of the parameter of smallness, $\frac{1}{Z}$. It is shown in the previous section that the graph (1) of figure 9 which gives the molecular field result is of order 1. But this result is obtained before the necessary renormalization is done to make the relation between β_c and $\frac{1}{Z}$ valid. In the renormalization process, all the g^0's are replaced by G^0's which are the result of summing all graphs of the form of graph (1) of figure 9. Thus, in this renormalized version of the graphs, all the graphs of the form of graph (1) and all their correction graphs are replaced by a simple G^0 line as in (2) of Fig. 9 which is still of order 1. The other graphs to be compared consist of two G^0's joined by one irreducible self-energy which contains complete G functions except where a Born approximation is applicable. This classification amounts to a classification of irreducible self-energies.

The two G^o's are included in determining the $\frac{1}{Z}$ order of the self-energy to take full account of the summation over indices at each end of the self-energy and to allow for the possibility of correction dotted lines involving the initial or terminal G^o. Only non-zero cases are considered. From the prescription given in the previous section, it is seen that all graphs considered except the simple G^o are of order higher than 1 in $\frac{1}{Z}$.

The only graph of order $\frac{1}{Z}$ is the graph (3) in figure 9 which comes from the transverse part of H_1. The interaction carries a $\frac{1}{Z}$ factor through β. It is possible to sum all the contributions to G_{ij} from graphs generated by the irreducible self-energy of this graph and thus obtain tne contributions to G(i,j) through order $\frac{1}{Z}$. This calculation is done in Appendix B.

The result is

$$G(i,j) = -\frac{1}{N}\sum_{q} e^{iq(r_i-r_j)}\, e^{-\{h+v(0)\ R-\frac{v(q)}{2}\tanh\frac{\beta}{2}[h+v(0)R]\}(\tau_i-\tau_j)} \times \tanh\frac{\beta}{2}[h+v(0)\ R] \begin{cases} \left[e^{-\beta\{h+v(0)\ R-\frac{v(q)}{2}\tanh\frac{\beta}{2}[h+v(0)R]\}}-1\right]^{-1} & \tau_i>\tau_j \\ \left[e^{+\beta\{h+v(0)\ R-\frac{v(q)}{2}\tanh\frac{\beta}{2}[h+v(0)R]\}}-1\right]^{-1} & \tau_i<\tau_j \end{cases} \tag{II2}$$

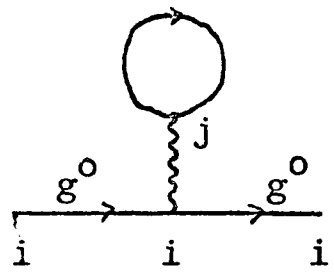
From this point on, it is understood that the internal lines appearing in the irreducible self-energies are renormalized to include at least all these graphs of order $\frac{1}{Z}$. Thus each of the internal lines

of the self-energies will be of the form of (3) in figure 9 or else of a form giving a higher order in $\frac{1}{Z}$. The use of $\frac{1}{Z}$ order internal lines in a self-energy of order $\frac{1}{Z^2}$ amounts to a Born approximation.

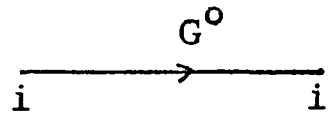
All the graphs of order $\frac{1}{Z^2}$ are of the form of the graphs (4) through (7) in figure 9. Graphs of the type of (5) are graphs generated by the $\frac{1}{Z}$ order irreducible self-energy but which have one correction dotted line whose delta function on site indices eliminates one summation. Graphs of the type of (5) are unlinked basic graphs from the transverse part of H_1 which are joined by one correction dotted line. And finally graphs of the form of (6) and (7) have parts from both the transverse and longitudinal terms of H_1. In general, it is not seen how to sum these graphs in which a correction dotted line appears. However, it is possible to sum them under approximations which are valid at low temperatures and at T_c. These cases are considered in Chapter III and IV. The result of the summation is then approximated for all temperatures in Chapter V.

All other graphs are of order higher than $\frac{1}{Z^2}$. These graphs involve more than one correction dotted line in the graphs from the transverse part of H_1 or more complicated combinations of transverse and longitudinal parts. Examplesof $\frac{1}{Z^3}$ graphs are given in (8) and (9) of figure 9.

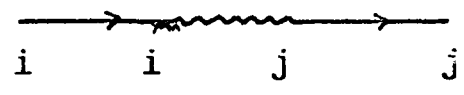
(1)



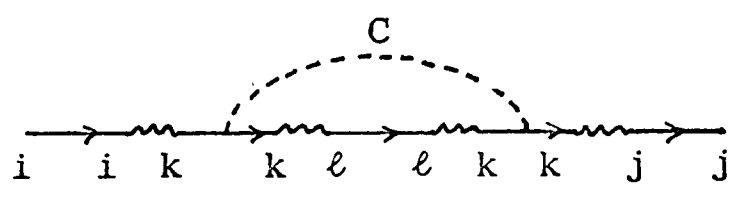
(2)



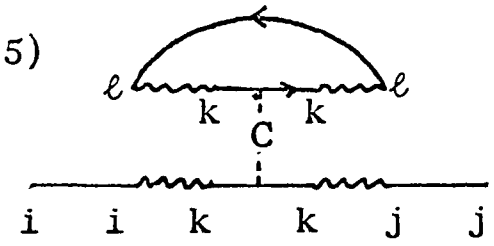
(3)



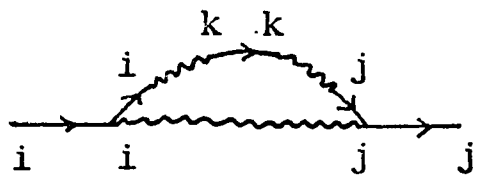
(4)



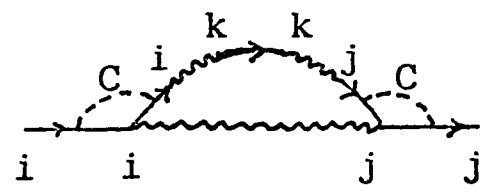
(5)



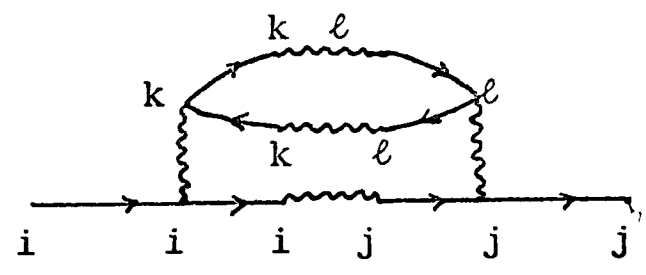
(6)



(7)



(8)



(9)

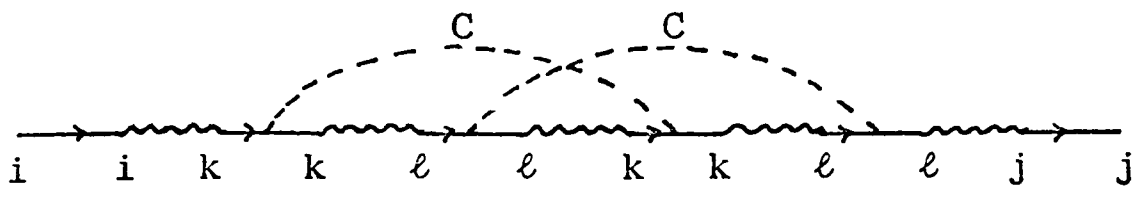


Figure 9

CHAPTER III

LOW TEMPERATURES

In this chapter the contributions to G through order $\frac{1}{z^2}$ are investigated at low temperatures and the resulting expression for the magnetization obtained. If the expansion for G is cut off at order $\frac{1}{z}$, then the expression for the magnetization

$$R = \tfrac{1}{2} - \frac{\tanh \frac{\beta}{2} [h+v(0)R]}{e^{\beta\{h+v(0)\ R - \frac{v(q)}{2} \tanh \frac{\beta}{2} [h+v(0)R]\}} - 1}, \qquad \text{(III1)}$$

given in Appendix B, leads at low temperatures to spin-wave theory with $T^{3/2}$, $T^{5/2}$ ... terms in the expression for the magnetization. It is shown in this chapter that including the order $\frac{1}{z^2}$ graphs leads in a Born approximation to Dyson's result for the low temperature magnetization which gives a T^4 rather than a T^3 correction to spin wave theory.

In Section A, the graphs of order $\frac{1}{z^2}$ are treated with a low temperature approximation which allows them to be summed. This summation is done and the result for the magnetization in Born approximation is compared to Dyson's expression. In section B, the terms in the expression for the magnetization are checked directly for their $\frac{1}{z}$ dependence using an argument about the range of $v(q)$. The $\frac{1}{z}$ ordering found is the same as the $\frac{1}{z}$ ordering justified for $\frac{\beta}{\beta_c}$ finite in Chapter II.

A. Contributions from Graphs through order $\frac{1}{Z^2}$

In this section, the contributions to G, and hence to R, are obtained from all the graphs through order $\frac{1}{Z^2}$ at low temperatures. The summation of all the graphs generated by the irreducible self-energy of order $\frac{1}{Z}$ is done in Appendix B, but, as it is stated in Chapter II, it is not seen how the graphs generated by the irreducible self-energies of order $\frac{1}{Z^2}$ may be summed in general. However, through an approximation valid at low temperatures, it is possible for the summation to be done. The approximation is a generalization to finite temperatures of the simplification made by Wang, Strikman and Callen (to be published) for T=0.

The approximation is based on the fact that for $T \rightarrow 0$ ($\beta \rightarrow \infty$) one of the factors of $G^0(i,i,\tau)$ is exponentially small for $\tau \leq 0$ and differs from -1 only by the same exponentially small term for $\tau > 0$. These conditions follow from equation II1. Thus, in the calculation of any quantity, such as the magnetization, which is expressed in a series in powers of T, the exponentially small parts of $G^0(i,i,\tau)$ may be neglected since they give contributions which approach zero faster than any finite power of T. From this approximation, it is possible to write $G^0(i,i;\tau_1,\tau_2)$ at low temperatures as

$$G^0(i,i;\tau_1,\tau_2) = - G^0(i,i;\tau_1,\tau_3)\, G^0(i,i;\tau_3,\tau_2) \,, \qquad \text{(III2)}$$

since the product of the phase factors associated with τ_3 is 1.

This expression can be used to simplify the summation of the graphs generated by the order $\frac{1}{Z^2}$ irreducible self-energies of the form of those in graphs (4) and (5) of figure 9.

If the time is plotted along the horizontal axis decreasing from left to right, the conditions on the times and indices implied by the correction dotted lines in one of the simplest cases of graphs (4) and (5) of figure 9 may be represented by the diagrams in figure 10.

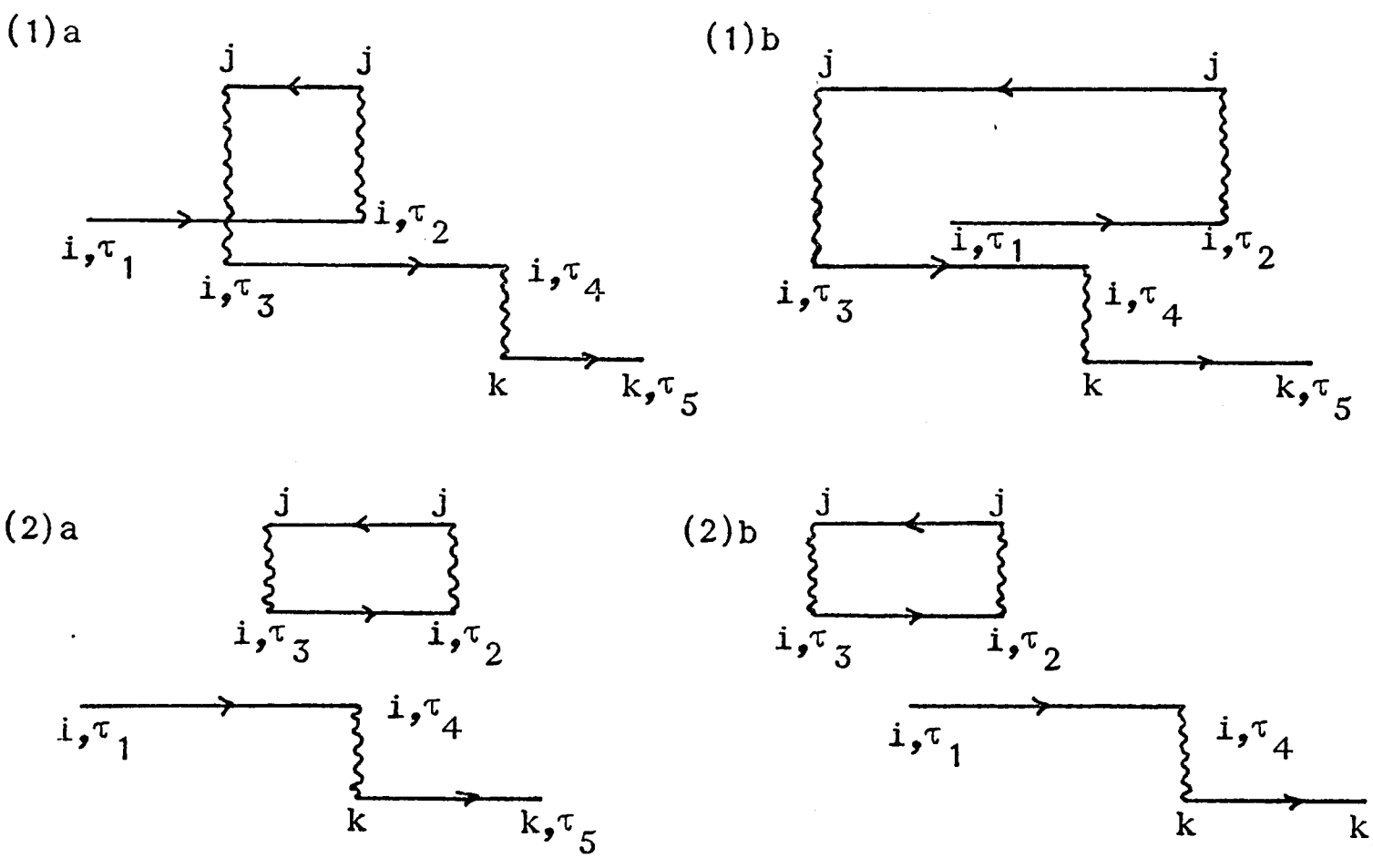


Figure 10

The overlapping of the lines of equal indices is considered fixed and only non-exponentially small time orders of the G^0's connected by the correction dotted lines are taken. The G^0 lines connected by the correction dotted lines have the same indices. Each diagram carries a factor of -2 from the correction dotted line.

The sum of the diagrams (1)a and (2)a of figure 10 is:

$$(1)a+(2)a= +2\int_{-\beta}^{\tau_1} d\tau_4 \int_{\tau_4}^{\tau_3} d\tau_2 \int_{\tau_4}^{\tau_1} d\tau_3\, G^o(i,i;\tau_1,\tau_2)\, G^o(i,i;\tau_3,\tau_4)\, G^o(j,j;\tau_2,\tau_3)$$

$$G^o(k,k;\tau_4,\tau_5)\, v_{ik} \sum_j v_{ij}^2 + 2\int_{-\beta}^{\tau_1} d\tau_4 \int_{-\beta}^{\tau_4} d\tau_2 \int_{\tau_4}^{\tau_1} d\tau_3\, G^o(i,i;\tau_1,\tau_4)$$

$$G^o(i,i;\tau_3,\tau_2)\, G^o(j,j;\tau_2,\tau_3)\, G^o(k,k;\tau_4,\tau_5)\, v_{ik} \sum_j v_{ij}^2 . \qquad \text{(III3)}$$

If the values of the G^o's are inserted, it is seen that the integrands are identical. Hence the sum is

$$(1)a+(2)a = +2\int_{-\beta}^{\tau_1} d\tau_4 \int_{-\beta}^{\tau_3} d\tau_2 \int_{\tau_4}^{\tau_1} d\tau_3\, G^o(i,i;\tau_1,\tau_4)G^o(i,i;\tau_3,\tau_2)G^o(j,j;\tau_2,\tau_3)$$

$$G^o(k,k;\tau_4,\tau_5)\, v_{ik} \sum_j v_{ij}^2 . \qquad \text{(III4)}$$

If the relation

$$G^o(i,i;\tau_1,\tau_4)= -G^o(i,i;\tau_1,\tau_3)\, G^o(i,i;\tau_3,\tau_4) \qquad \text{(III5)}$$

is used in equation III4, then

$$(1)a+(2)a = +2\int_{-\beta}^{\tau_1} d\tau_4 \int_{-\beta}^{\tau_3} d\tau_2 \int_{\tau_4}^{\tau_1} d\tau_3\, G^o(i,i;\tau_1,\tau_3)G^o(i,i;\tau_3,\tau_4)G^o(i,i;\tau_3,\tau_2)$$

$$G^o(j,j;\tau_2,\tau_3)G^o(k,k;\tau_4,\tau_5)\, v_{ik} \sum_i v_{ij}^2 \qquad \text{(III6)}$$

which may be represented by diagram (1) in figure 11.

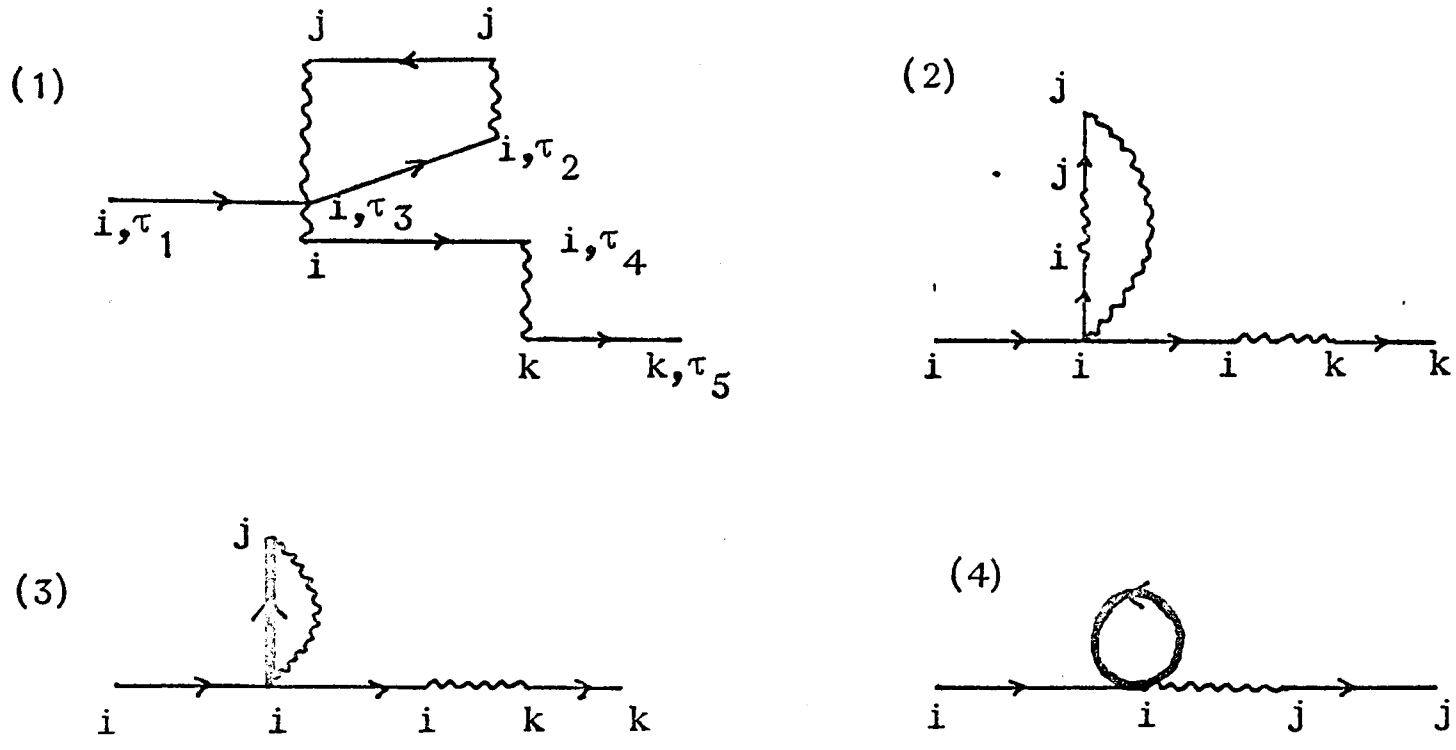


Figure 11

In the diagram it is understood that τ_2 may be both less than and greater than τ_4. In fact, it is seen that the integrations over τ_2 and τ_3 may be done over the whole range $-\beta$ to $+\beta$ since the part of this range missing in equation III6 gives exponentially small contributions from the $G^o(i,i)$'s. Thus the sum in equation III6 may be represented in the style of the graphs introduced in Chapter I by graph (2) of figure 11 where all the internal integrations over time go from $-\beta$ to $+\beta$.

It is clear that the loop in graph (2) of figure 10 could be of any size since graphs of order $\frac{1}{Z}$ with several interaction terms could appear instead of the simple $G^o(j,j)$. If the sum of all these $\frac{1}{Z}$ order graphs is put into the loop, the result of this renormalization is represented by graph (3) of figure 11. The bold line represents the sum of the contributions of all graphs through order $\frac{1}{Z}$ to $G(i,j;\tau_i=\tau_j) = -n_{ij}$. This sum is taken to be $-n_{ij}$ in a Born approximation. It is noted that the loop does not appear in the form which would give the simple $G^o(i,j;\tau_i=\tau_j)$ contribution to n_{ij}. But the absence of this term does not matter because

$G^{o}(i,j)$ for $i \neq j$ is always zero.

Also it is seen that the loop represents an irreducible self-energy corresponding to parts of both of the irreducible self-energies of the graphs of the form of graphs (4) and (5) of figure 9. This new irreducible self-energy may be used in Dyson's equation as usual. Detailed illustrations of how Dyson's equation becomes algebraic through Fourier transformation and how the irreducible self-energy is picked out are given in Appendices A and B. If graph (3) of figure 10 is Fourier transformed according to equation B3 in Appendix B, the new irreducible self-energy is found to be

$$\sum^{(1)} = + \sum_{q'} n(q')\, v(q') \; . \qquad \text{(III7)}$$

The factor of 2 coming from the correction dotted line is canceled by the factor of ½ associated with the exchange integral v_{ij} or its Fourier component $v(q')$.

In exactly the same manner as that used to treat graphs (1)a and (2)a of figure 10, it can be shown that graphs (1)b and (2)b of figure 10 lead to graph (4) of figure 11. In this graph, the bold line loop contains the sum of all the contributions to $G(i,i;\tau_1=\tau_2)$ from graphs through order $\frac{1}{Z}$ except for the simple $G^{o}(i,i;\tau_1=\tau_2)$. This time the missing contribution is not zero but is given by $\dfrac{1}{e^{\beta[h+v(0)R]} + 1}$. The sum of all the contributions to $G(i,i;\tau_1=\tau_2)$ through order $\frac{1}{Z}$ is taken to be $G(i,i;\tau_1=\tau_2)$ in a Born approximation, and the loop is expressed as:

$$G(i,i;\tau_1=\tau_2) - G^0(i,i;\tau_1=\tau_2) = \bar{n} - \frac{1}{e^{\beta[h+v(0)R]} + 1} \quad . \tag{III8}$$

If the graph (4) of figure 11 is Fourier transformed in the manner used for graph (3) of figure 11 and the irreducible self-energy picked out, it is seen that

$$\sum^{(2)} = + \left\{ \bar{n} - \frac{1}{e^{\beta[h+v(0)R]} + 1} \right\} v(q) \quad . \tag{III9}$$

At low temperatures, the second term in the first factor may be neglected and $\Sigma^{(2)}$ expressed as:

$$\sum^{(2)} = + \bar{n}\, v(q) \quad . \tag{III10}$$

Again the factor 2 coming from the correction dotted line is canceled by the factor ½ associated with the exchange integral.

The remaining graphs of order $\frac{1}{Z^2}$ are graphs of the form of (6) and (7) of figure 9. In graph (7), both cases of the two G^0 lines connected by a correction dotted line give terms which are exponentially small at low temperatures. The three possible cases of overlap implied by the correction dotted line are shown in figure 12 where time is plotted along the horizontal axis decreasing from left to right.

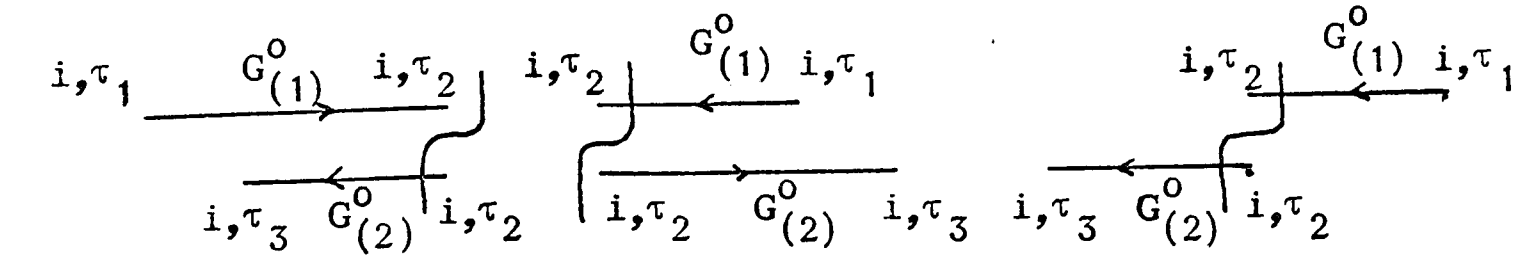


Figure 12

The S_i^- operator of $G^o_{(1)}$ and the S_i^+ operator of $G^o_{(2)}$ have the same times; so, the S_i^- operator is always taken on the left of the S_i^+ operator. In graph (1) of figure 12, $G^o_{(2)}$ has an exponentially small term, in Graph (2), $G^o_{(1)}$ has an exponentially small term, and in graph (3), both G^o's have exponentially small terms. Thus at low temperatures, graphs of the form of graph (7) of figure 9 may be neglected.

Graphs of the form of graph (6) of figure 9 may be represented by the graph of figure 13. Two graphs of this form actually appear in the expansion differing only by an interchange of the indices at the ends of the interaction. Since these indices are summed over, the contributions are the same. Thus one graph with a factor of 2 is taken. The graph carries a plus sign in front of it.



Figure 13

The bold line represents the sum of the contributions of all the graphs through order $\frac{1}{Z}$ to $G(i,i;\tau_i=\tau_j) = -n_{ij}$. Again, the $G^o(i,j)$ graph is missing, but its contribution is always zero. This bold line is taken to be $-n_{ij}$ in a Born approximation. If the graph of figure 13 is Fourier transformed in the usual manner, it is seen that its irreducible self-energy is:

$$\sum^{(3)} = - \sum_{q'} n(q')\, v(q-q') \,. \qquad \text{(III11)}$$

The multiplicative factor of 2 is canceled by the factor $\frac{1}{2}$ associated with the exchange integral.

All of the graphs generated by the order $\frac{1}{Z^2}$ self-energies at low temperatures and by the $\frac{1}{Z}$ order self-energy of Appendix B may be summed using Dyson's equation. It is noted in Appendix B that under Fourier transformation Dyson's equation becomes algebraic

$$G(q,\omega_n) = G^0(q,\omega_n) + G^0(q,\omega_n) \sum(q,\omega_n)\, G(q,\omega_n) \qquad (B2)$$

with

$$G^0(q,\omega_n) = \frac{\tanh \frac{\beta}{2}\,[h+v(0)R]}{i\omega_n - h - v(0)R} \qquad \text{and} \qquad \omega_n = \frac{2n\pi}{\beta}\ .$$

The Fourier transformed irreducible self-energy of order $\frac{1}{Z}$ from Appendix B is $\Sigma(q,\omega_n) = \frac{-v(q)}{2}$, and at low temperatures the ones of order $\frac{1}{Z^2}$ are, from this section,

$$\sum^{(1)} = \sum_{q'} n(q')\, v(q'), \quad \sum^{(2)} = \bar{n}\, v(q) \quad \text{and} \quad \sum^{(3)} = -\sum_{q'} n(q')\, v(q-q')\ .$$

The Σ appearing in Dyson's equation is the sum of these self-energies

$$\sum(q,\omega_n) = -\,R\, v(q) + \sum_{q'} n(q') \Big[v(q') - v(q-q') \Big]. \qquad (III12)$$

Inserting this expression for $\Sigma(q,w_n)$ into equation B2 yields

$$G(q,\omega_n) = \frac{\tanh \frac{\beta}{2}\,[h+v(0)R]}{i\,\omega_n - h - v(0)R + \left\{ + v(q)R - \sum_{q'} n(q') \Big[v(q') - v(q-q') \Big] \right\} \tanh \frac{\beta}{2}\,[h+v(0)R]} \qquad (III13)$$

From Appendix B

$$G(i,j) = \frac{1}{N} \sum_{q} \frac{1}{\beta} \sum_{\omega_n} G(q,\omega_n)\, e^{iq.r_i - r_j}\, e^{-i\omega_n(\tau_i - \tau_j)} \quad . \tag{B4}$$

Thus, to obtain G(i,j), equation III13 is inserted into equation B4. The sum over all the ω_n may be done by converting the summation into a contour integration exactly as is done in Appendix A for the case of n even. The result is

$$G(i,j) = -\frac{1}{N} \sum_{q} e^{iq.(r_i - r_j)} \exp\left\{-g(q)\,[\tau_i - \tau_j]\right\} \times \tanh\frac{\beta}{2}[h+v(0)R]$$

$$\times \begin{cases} \left[\exp(-\beta\, g(q)\,) - 1\right]^{-1} & \tau_i > \tau_j \\ \left[\exp(+\beta\, g(q)\,) - 1\right]^{-1} & \tau_i \leq \tau_j \end{cases} \tag{III14}$$

where

$$g(q) = +h+v(0)R + \left\{- v(q)R + \sum_{q'} n(q') \left[v(q) - v(q-q')\right]\right\} \tanh\frac{\beta}{2}[h+v(0)R] \quad .$$

The magnetization is given by

(III15)

$$\bar{R} = \tfrac{1}{2} + G(i,i;\tau=0) = \tfrac{1}{2} - \frac{1}{N} \sum_{q} \frac{1}{\exp\left\{\beta\left[+h+[v(0)-v(q)]R + \sum_{q'} n(q')[v(q')-v(q-q')]\right]\right\} - 1}$$

where the $\tanh\frac{\beta}{2}[h-v(0)R]$ factors have been set equal to 1 since they differ from 1 only by exponentially small terms at low temperatures.

It is noted especially that $\tanh \frac{\beta}{2} [h+v(0)R]$ is the factor coming in the numerator of the second term in equation III15 and that this term may be set equal to 1 at low temperatures as is done. Expressions coming from RPA would have a simple 2R in place of the "tanh" function and, of course, this 2R may not be approximated by 1 at low temperatures. Equation III15 is equivalent to Dyson's first Born approximation for the magnetization and yields a T^4 rather than a T^3 correction to spin wave theory.

B. Direct Check on $\frac{1}{Z}$ Ordering

In this section, the terms in equation III15 for the magnetization are checked directly for their $\frac{1}{Z}$ order using an argument based on the $\frac{1}{Z}$ dependence of the range of v(q) and on the known temperature dependencies of the terms. It is seen that the $\frac{1}{Z}$ ordering of the terms is in agreement with the $\frac{1}{Z}$ ordering of the irreducible self-energies giving rise to the terms.

From Bloch (1930,32) it is known that at low temperatures $\sum_{q'} n(q')$ is proportional to $T^{3/2}$ plus other terms of higher powers of T. Thus, it is possible to expand equation III15 for the magnetization in terms of $\sum_{q'} n(q')$ in the following manner.

$$R = \tfrac{1}{2} - \frac{1}{N} \sum_{q} \frac{1}{e^{\frac{\beta}{2}[v(0)-v(q)]} - 1} + \frac{1}{N} \sum_{q} \frac{e^{\frac{\beta}{2}[v(0)-v(q)]} \sum_{q'} n(q') [v(q')-v(q-q') + v(q) - v(0)]}{\left(e^{\frac{\beta}{2}[v(0)-v(q)} - 1\right)^2} + \ldots \qquad \text{(III16)}$$

with $h \longrightarrow 0$.

The $\frac{1}{Z}$ ordering is introduced into this equation through the summations over the Brillouin zone of q and q': If $v_{ij}=v(\mathbf{r})$ has a range beyond which it is negligible given by $Z = {}^{4}/_{3}\,\pi\, r_o^3\,\rho$, $r_o = \left(\frac{Z}{{}^{4}/_{3}\,\pi\,\rho}\right)^{1/3}$, then v(q) is taken to have a range q_o given by $q_o = \frac{2}{r_o}$. Hence $q_o = \frac{2}{a}\left(\frac{{}^{4}/_{3}\,\pi}{Z}\right)^{1/3}$ where $a = \frac{1}{\rho^{1/3}}$ is the lattice spacing. The ratio of the number of terms with $q \lesssim q_o$ in the sum over the Brillouin zone to the total number of terms in the sum is

$$\frac{N_{q\lesssim q_o}}{N} = \frac{{}^{4}/_{3}\,\pi\, q_o^3}{\left(\frac{2\pi}{a}\right)^3} = \frac{16}{9\pi Z} \quad . \tag{III17}$$

Thus

$$N_{q\lesssim q_o} = \frac{16\,N}{9\pi\,Z} \; ; \quad N_{q>q_o} = N\left(1 - \frac{16}{9\pi Z}\right) . \tag{III18}$$

In the second term of equation III16, the number of terms in the summation for which $q \lesssim q_o$ and hence, for which v(q) appears in the exponential is proportional to $\frac{N}{Z}$ from equation III18. The terms in the sum for which $q > q_o$, are exponentially small at low temperatures and may be neglected. Thus the second term in equation III6 gives a contribution to R proportional to $\frac{1}{Z}$. This contribution is the one associated with the appearance of the energy $\frac{-v(q)}{2}$ which comes from the irreducible self-energy of Appendix B found to be of order $\frac{1}{Z}$.

If this second term of equation III16 is used for $\sum_{q'} n(q')$ in the third term in a Born approximation, it is seen in the same manner as above that in each of the summations over q and q' the number of terms which are

not exponentially small at low temperatures is proportional to $\frac{1}{Z}$. Hence the whole term is proportional to $\frac{1}{Z^2}$. Under a particular summation the interaction terms in the last factor of the numerator of this third term either cut off at the same place or near the same place one of the other factors becomes exponentially small or remain constant. In either case, they themselves do not directly affect the determination of the $\frac{1}{Z}$ order of the term. Thus the term associated with the energies $\Sigma_{q'} n(q') [v(q')-v(q-q')+v(q)-v(0)]$ is found to give a contribution to R at low temperatures proportional to $\frac{1}{Z^2}$. These energies are just those coming from the irreducible self-energies of order $\frac{1}{Z^2}$ in Chapter II. It should be noted that whereas the term $v(0)\,\bar{n}=v(0)\,\Sigma_{q'} n(q')$ is first introduced in order 1, it appears in this section with an order $\frac{1}{Z^2}$ part since the loop giving rise to the $\bar{n}$ is always renormalized with all the graphs considered. Since graphs through order $\frac{1}{Z^2}$ are summed to obtained the expression for R in equation III15, there will be graphs of order $\frac{1}{Z^2}$ in the loop and hence an order $\frac{1}{Z^2}$ contribution from this term in the magnetization.

Thus it is seen that the $\frac{1}{Z}$ ordering of the contributions to G, and hence to R, justified for $\frac{\beta}{\beta_c}$ finite is found to hold at low temperatures also.

CHAPTER IV

CURIE TEMPERATURE

As it is stated in the introduction, the RPA expression for the magnetization decreases monotonically as the temperature is increased from zero, until its zero field value is zero for all temperatures beyond a well defined critical temperature. The critical temperature is that of the spherical model of Berlin and Kac (1952). Also, the renormalized version of the work of Stinchcombe et al.(1963) yields a critical temperature, that of molecular field theory. Both of these theories give expressions for the magnetization which for h=0 have numerators and denominators proportional to R in the limit of small R. Thus, the limit is well defined, and an equation for the Curie temperature is obtained directly.

The results of these two theories differ from those which M. Bloch (1962) finds when she tries to extend Dyson's low temperature results to the Curie point. The expression for the magnetization used in this case does not have a direct limit obtained by letting R tend to zero, and so the number of spin waves excited at the temperature increases is determined self-consistently using a computer. However, the solution for the magnetization becomes double valued as it approaches the Curie temperature indicating that the magnetization makes a discontinuous jump to zero at the Curie point.

The expressions for the magnetization given in this chapter, both through order $\frac{1}{Z}$ and through order $\frac{1}{Z^2}$, have limits as R tends to zero in the manner of the expressions of RPA and Stinchcombe et al. since the order 1 graphs are renormalized to include in their internal lines all graphs of other orders appearing later. Thus there is no discontinuous jump in the magnetization as it approaches zero, and the equation for β_c is obtained directly. The terms through order $\frac{1}{Z}$ yield the Curie temperature of molecular field theory, but a condition on the potential which is not necessarily true is also found. This discrepancy is removed when the terms through order $\frac{1}{Z^2}$ are included, and the Curie point of molecular field theory is obtained in a consistent manner.

In Section A, the results from graphs through order $\frac{1}{Z}$ are briefly given since they are the same as those found by Stinchcombe et al. in that order. In Section B, the $\frac{1}{Z^2}$ graphs are treated, and it is seen that conditions holding at the Curie temperature make some of the $\frac{1}{Z^2}$ graphs zero and allow others to be summed.

A. Curie Point from Graphs Through Order $\frac{1}{Z}$

The expression for the magnetization from graphs generated by the order $\frac{1}{Z}$ irreducible self-energy, $-\frac{v(q)}{2}$ is given in Appendix B as

$$R = \tfrac{1}{2} - \sum_q \frac{\tanh \frac{\beta}{2}\left[h+v(0)\ R\right]}{e^{\beta\{h+v(0)\ R - \frac{v(q)}{2}\tanh\frac{\beta}{2}\left[h+v(0)\ R\right]\}} - 1} . \qquad \text{(B6)}$$

In the limit of $h \to 0$, the susceptibility, $\frac{\partial R}{\partial h}$, diverges at the molecular field theory Curie temperature, $\beta_c = \frac{4}{v(0)}$. However, taking the limit of R and h going to zero in equation B6, leads to a condition on the

potential, $1 = \frac{1}{N} \sum_q \frac{v(0)}{v(0)-v(q)}$, where the molecular field theory expression for β_c is used. This condition on the potential is not necessarily true. Stinchcombe et al. (1963) eliminate this by including other graphs in a renormalization scheme and obtain the molecular field Curie point in an approximation on these more complicated graphs. In the next section it is shown that the difficulty in the $\frac{1}{Z}$ order Curie point of this thesis is eliminated by including the $\frac{1}{Z^2}$ graphs and that the Curie point of molecular field theory is obtained consistently.

B. Curie Point from Graphs Through Order $\frac{1}{Z^2}$

In this section, the contributions of the graphs generated by the irreducible self-energies of order $\frac{1}{Z^2}$ are included in the expression for the magnetization near the Curie temperature. Because of a special condition holding at the Curie point, either these graphs cancel each other or else they may be summed. This condition is that at β_c and for $h \rightarrow 0$, G^o has the same value, apart from the phase factors, for both time orders. The second factor in equation II1 is always ½. Thus, the equation

$$G^o(\tau_1,\tau_2) = -2\, G^o(\tau_1,\tau_3)\, G^o(\tau_3,\tau_2) \qquad \text{IV1)}$$

holds. This equation differs from the corresponding equation at low temperatures only by a factor 2. The graphs generated by the irreducible self-energies of $\frac{1}{Z^2}$, which are of the form of graphs (4),(5),(6) and (7) of figure 9, may be simplified using these conditions near β_c.

The dotted line graph giving rise to all the graphs of the form of (6) and (7) of figure 9 is shown in figure 14. As it is stated in Chapter I, the dotted line does not restrict the ranges of integration as the correction dotted line does.

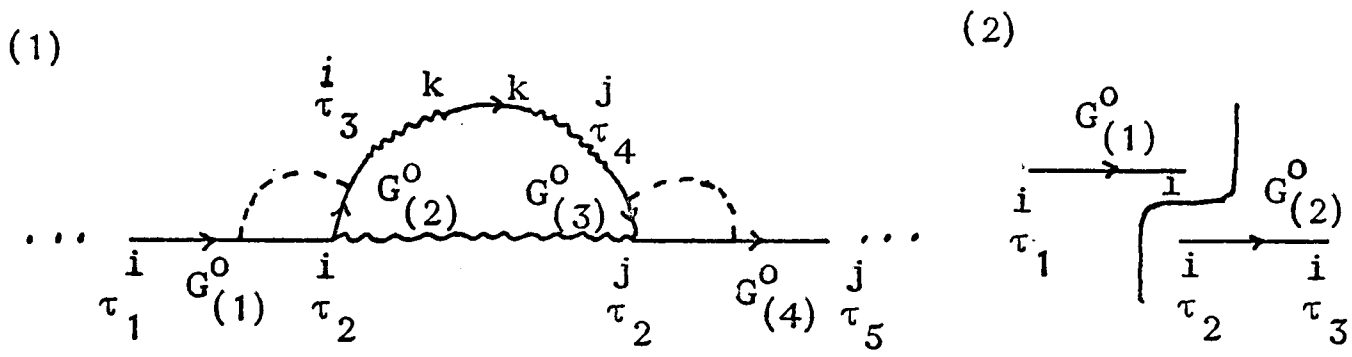


Figure 14

The integrations are over the whole range $-\beta$ to β, but a minus sign is taken if the terms of the G^o's connected by the dotted lines overlap. The three dots on eacn end of the graph indicate that in the general case this graph appears with other graphs attached on eacn end. Thus τ_1 and τ_5 are in general integrated from $-\beta$ to β also. The sign of the graph must not depend on the relations between τ_1 and τ_5 and times appearing in the graphs attached on eacn end, for then a higher order irreducible self-energy would be involved. Also, all the internal phase factors associated with these G^o's cancel.

If all the times are fixed in the graph except τ_1 and τ_3, then the integrations over τ_1 and τ_3 give exactly canceling positive and negative contributions. This fact is seen as follows. If τ_1 and τ_3 have the relationship implied by graph (2) of figure 14 where time is plotted along the horizontal axis, the contribution to the integrals is plus. The S^- operator in $G^o_{(1)}$ and the S^+ operator in $G^o_{(2)}$ have the same times. Therefore, the S^- is taken to the left of the S^+ and the G^o's do not overlap. However, if the contribution to the integrals in taken with τ_1 and τ_3 just interchanged, the G^o's overlap, the sign is minus, and this contribution exactly cancels the positive contribution because the value of the G_o's without the phase factors is the same regardless of the time order. The result holds for τ_1 and τ_3 regardless of their relation to τ_2. Thus every positive contribution to the integrals is canceled by a negative one and the graph is zero. The same result would be obtained if τ_4 and τ_5 were considered. If either τ_1 or τ_5 is fixed, the result is the same from considering the one that is not fixed. They are both fixed only when the graph stands alone. In that case i is set equal to j to get the magnetization, and the graph is zero since i may not equal the j across an interaction. Thus all the graphs of the form of graphs (6) and (7) of figure 9, which account separately for the contributions from different parts of the ranges of the integrations in graph (1) of figure 14, cancel each other and need not be considered at the Curie point.

The graphs of the form of graphs (4) and (5) of figure 9 do not cancel at the Curie point, but they may be considerably simplified. Some of the possible time orderings of these graphs are shown in

figure 10 where time is plotted along the horizontal axis. These graphs are the set of time orders giving corrections if $\tau_1 > \tau_4$. It should be noted that in this case of $\beta=\beta_c$, graphs 2(a) and 2(b) also give corrections if τ_2 and τ_3 are interchanged since the G^o's with the times interchanged are no longer exponentially small. Likewise, there exists another set of four graphs corresponding to the four graphs of figure 10 but with $\tau_4 > \tau_1$. These graphs are all exponentially small at low temperatures, but are just as important as those of figure 10 at β_c. Because the G^o's at β_c have the same value apart from phase factors for both time orderings, the expressions for these eight graphs have the same integrands since the phase factors cancel. The expressions differ only in their ranges of integration.

All these graphs may be added together in pairs just as is done for the pair 1(a) and 2(a) at low temperatures. The sum of 1(a) and 2(a) again gives the graph (1) of figure 11 where equation IV1 is used in the way equation III5 is used at low temperatures. In addition to the condition on the times of this graph at low temperatures, τ_2 and τ_3 may be interchanged if τ_2 is greater than τ_4. This new possibility comes from the fact noted above that τ_2 and τ_3 may be interchanged in graph 2(a) of figure 10. The graph also carries a factor of 2 from the use of equation IV1. Graphs similar to graph (1) of figure 11 are obtained from adding together in pairs the other graphs of figure 10 and the new set of four graphs corresponding to them but with τ_1 less than τ_4.

These four graphs again have identical integrands but differ in the ranges of integration. For certain values of τ_1 and τ_4, the ranges of integration of these four graphs add up to exactly ½ the full range of

integration obtained by integrating all times from $-\beta$ to $+\beta$. In the other cases of τ_1 and τ_4, the sum of the ranges differs from ½ the full range by a small fraction. Hence, the four graphs are added together, the integrations of the resulting expression performed over the full ranges, and the expression multiplied by ½. This approximation leads to a result which is formally the same as that obtained by Stinchcombe et al. (1963) using the excluded volume approximation of Brout (1961).

The loops appearing in the four graphs of the form of graph (1) of figure 11 could be of any size. Hence, the graph representing the sum of these four graphs is the graph of figure 15 where the bold line represents the sum of all contributions to $G(i,j;\tau_i=\tau_j)$.

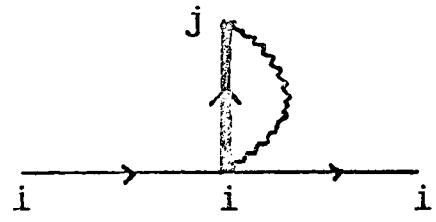


Figure 15

The integrations over times in the graph are all from $-\beta$ to $+\beta$. The factor of ½ coming from the extension of the ranges of integration is canceled by the factor of 2 coming from the use of equation IV1.

In the same manner used in Section A of Chapter II, it can be shown that the irreducible self-energy associated with the graph in figure 15 is

$$\sum = + \sum_{q'} n(q')\, v(q') \ . \qquad \text{(IV2)}$$

This is the only irreducible self-energy of order $\frac{1}{Z^2}$ appearing at β_c. If this self-energy is put into Dyson's equation for $G(i,j)$ along with the irreducible self-energy of order $\frac{1}{Z}$, the expression for the magnetization

at β_c, obtained in the manner of Appendix A for periodic G's, is

$$R=\tfrac{1}{2} + G(i,i,\tau=0^-)=\tfrac{1}{2}- \frac{1}{N} \sum_q \frac{\tanh \frac{\beta}{2}[h+v(0)R]}{e^{\beta\{h+v(0)R - [\frac{v(q)}{2} - \sum_{q'} n(q')v(q')]\tanh \frac{\beta}{2}[h+v(0)R]\}} -1} \tag{IV3}$$

If h is set equal to zero in this equation for R and the limit as R approaches zero is taken, the following condition between β_c and δ_c is obtained,

$$1 = \frac{1}{N} \sum_q \frac{1}{1 - \frac{\beta_c}{4}[v(q) - \delta_c]} , \tag{IV4}$$

where $\delta = 2 \sum_{q'} n(q')v(q')$. Since δ is independent of q, it is possible to check this equation for consistency.

$$\beta_c\delta_c = \beta_c \frac{2}{N} \sum_{q'} n(q')\, v(q') = \frac{2}{N} \sum_{q'} \frac{\frac{\beta_c}{2} v(q')}{1 - \frac{\beta_c}{4}[v(q')-\delta_c]}$$

$$= \frac{4}{N} \sum_{q'} \left\{ \frac{\frac{\beta_c}{4}[v(q')-\delta_c] - 1 + \frac{\beta_c}{4}\delta_c + 1}{1 - \frac{\beta_c}{4}[v(q')-\delta_c]} \right\} = \beta_c\delta_c \tag{IV5}$$

where equation IV4 is used to make the last step.

In Chapter V, the expressions for the magnetization at low temperatures and at β_c are used as a guide in approximating the contributions to the magnetization through order $\frac{1}{Z^2}$ for all temperatures. The result is given in equation V3. Determining from this equation the temperature at

which the susceptibility ~~diverges~~ χ diverges in the limit of zero field gives another equation for β_c. To accomplish this, equation V3 is expanded to obtain all terms through first order in h. The result is

$$R=\tfrac{1}{2} - \frac{1}{2N} \sum_{q} \frac{1 - \frac{\beta}{2}\{h+v(0)R\}\left\{1-\beta\left(\frac{v(q)-\delta}{4}\right)\right\} - \frac{\beta^2}{8}[h+v(0)R]v(q) - \frac{\beta}{2} R\, v(q)}{1-\beta\left(\frac{v(q)-\delta}{4}\right)}}{1 - \beta\left(\frac{v(q)-\delta}{4}\right)} \qquad \text{(IV6)}$$

since R may be written as $R=\chi h$ for small h and R. Differentiating this equation with respect to h and taking the limit of h going to zero then yields an expression for χ which diverges at $\frac{\beta_c v(0)}{4} = 1$. Thus the molecular field theory Curie point is obtained, and this result is consistent with equation IV4.

It is noted that for the Ising model, Horwitz and Callen (1961) obtain an improvement on the molecular field Curie point equation by a consistent renormalization of the rings appearing in their expansion. This procedure leads to a translation of v(0) to a term of the form v(0)+u. A result of this form would be obtained from the expansion of this thesis in the following manner. Dropping the transverse part of H_1 leaves just the Ising Hamiltonian. The expansion for the Green's function may now be made and the graphs summed in exactly the same manner as for the molecular field graphs of Appendix A. The T operator appears everywhere and there are no correction dotted lines since the operators in H now appear in equal-index, equal-time pairs. The consistent renormalization of Horwitz and Callen corresponds to taking now certain

irreducible self-energies, using complete Green's functions in the internal lines, and then summing all the graphs generated by the self-energies using Dyson's equation. The self-energies are chosen by considering the $\frac{1}{Z}$ order of their "skeleton" graphs or the graphs with G^0's appearing. Then the internal lines of the self-energies of the respective $\frac{1}{Z}$ orders are made complete Green's functions in the renormalization process. It is noted that this is precisely the procedure followed in Appendix A of this thesis where the molecular field theory result is obtained.

For the Ising model, Horwitz and Callen are also able to include the completely renormalized $\frac{1}{Z}$ graphs, which are their ring graphs. This corresponds exactly to including the sum of all graphs of the form of graph 8 of figure 9 without any transverse parts and with complete Green's functions in the internal lines of the self-energies. The explicit calculation of the sum of these graphs as well as higher order graphs would be a useful application of the expansion technique of this thesis to the Ising Model.

To be consistent in the Heisenberg model, the skeleton graphs of the respective orders of $\frac{1}{Z}$ from the transverse part of H must be included in the same way as the skeleton graphs from the longitudinal part of H. And once the transverse part of H is included, correction dotted lines appear in both the longitudinal and transverse graphs. Because of the complications introduced by the dotted lines, it is seen how to treat these self-energies only for the case of $\frac{1}{Z}$ order graphs appearing in their internal lines and not for their completely renormalized version. When these self-energies involving dotted lines are included, the Curie point of molecular field theory is still obtained since the molecular field theory graphs are the only ones completely renormalized.

CHAPTER V

APPROXIMATION OF $\frac{1}{Z^2}$ CONTRIBUTIONS TO MAGNETIZATION AT ALL TEMPERATURES; COMPARISON TO EXPERIMENT

In this chapter the expressions for the magnetization given in Chapter III for low temperatures and in Chapter IV for β_c are used as a guide in approximating the $\frac{1}{Z^2}$ contributions to $\langle S_z \rangle$ at all temperatures. The resulting theoretical curve is compared to experimental results for the magnetization of a ferromagnetic insulator of spin ½ which has longer ranged interactions than just nearest neighbor. The theoretical magnetization curve given by RPA is also compared to the experimental results. In calculating both of the theoretical curves, an approximation is made on v(q) which is valid for a long range potential. Both of the theoretical curves fit the experimental curves at low temperatures; however, as β_c is approached, both curves dip below the experimental points. The difference between the two theoretical curves in this region is negligible.

In Section A the approximation on the $\frac{1}{Z^2}$ contribution is made. The experimental results are presented in Section B, and the theoretical magnetization curves from the approximate formula of this thesis and also from RPA are calculated and compared to these experimental results in Section C.

Section A Approximation of $\frac{1}{Z^2}$ Contributions at All Temperatures

In this section, the expressions for the magnetization given in Chapter III for low temperatures and in Chapter IV for β_c are used as a guide in approximating the $\frac{1}{Z^2}$ contributions to $\langle S_z \rangle$ at all other temperatures.

These expressions are

$$R=\tfrac{1}{2} - \frac{1}{N} \sum_{q} e^{\frac{1}{+\beta\{+h+[v(0)-v(q)]R + \sum_{q'} n(q')[v(q')-v(q-q')]\}}} - 1 \qquad (V1)$$

at low temperatures with the exponentially small terms neglected and

$$R=\tfrac{1}{2} - \frac{1}{N} \sum_{q} \frac{\tanh \frac{\beta}{2}[h+v(0)R]}{+\beta\left\{+h+v(0)R - \left[\frac{v(q)}{2} - \sum_{q'} n(q')v(q')\right]\tanh \frac{\beta}{2}[h+v(0)R]\right\}} \qquad (V2)$$

$$e \qquad -1$$

at β_c. The tanh factors in the latter expression become 1 at low temperatures and the two expressions differ only in their energies. The difference in the energies comes from the fact that the irreducible self-energies of order $\frac{1}{Z^2}$ differ under the low temperature approximation used in Chapter III and under the approximation used at β_c. It is these expressions for the irreducible self-energies of order $\frac{1}{Z^2}$ which are now approximated at all other temperatures, and the approximate formula for the magnetization is found from them.

The order $\frac{1}{Z^2}$ self-energies at low temperatures are, from Chapter III, $+\sum_{q'} n(q')v(q')$, $+\left(\bar{n} - \frac{1}{e^{\beta[h+v(0)R]}+1}\right) v(q)$, and $-\sum_{q'} n(q')\, v(q-q')$, and the only order $\frac{1}{Z^2}$ irreducible self-energy at β_c is, from Chapter IV, $\sum_{q'} n(q')v(q')$. It is noted that this single self-energy at β_c appears both at low temperatures and at β_c and no approximation on it is made. Also, the self-energy $\left(\bar{n} - \frac{1}{e^{\beta[h+v(0)R]}+1}\right)\times$ $v(q)$ at low temperatures is seen to vanish at β_c in the limit of $h \to 0$, since both $\bar{n}$ and $\frac{1}{e^{\beta\, v(0)R}+1}$ equal ½ at β_c. Therefore, no approximation coefficient is added to this term.

However, it is necessary to multiply the self-energy $-\sum_{q'} n(q')v(q-q')$ by a coefficient which equals 1 in the limit of $T \to 0$ and equals zero at β_c. This self-energy is of the form of those of graphs (5) and (6) of figure 9 in Chapter II, and the manner in which it vanishes at β_c is discussed in connection with figure 14 in Chapter IV. In the discussion in Chapter IV, it is seen that the vanishing of the graph stems from the fact that at β_c the G^0's have the same values, apart from phase factors, for both time orders. The integrand in the expression for graph (1) of figure 14 does not change for different time orders, but the sign in front of the integral does. The positive and negative contributions cancel at β_c. However, as the temperature is lowered from T_c, the G^0's do not have the same values for each time order, and the positive and negative parts fail to cancel by an amount depending on the difference of the G^0's for the two time orders. Since this difference is a difference between exponential terms which is zero at β_c and goes to 1 at low temperatures, $\tanh^2 \frac{\beta}{2}[h+v(0)R]$ is the interpolation coefficient

chosen. The tanh function is taken to the second power since the graph (1) of figure 14 has the same cancellation at β_c from considering either end of the graph. Thus the low temperature self-energy $\Sigma_{q'} n(q')v(q-q')$ is approximated at all temperatures by

$$\tanh^2 \frac{\beta}{2}[h+v(0)R] \sum_{q'} n(q')v(q-q').$$

If this self-energy and the self-energies $\Sigma_{q'} n(q')v(q')$ and $\left[\bar{n} - \frac{1}{e^{\beta[h+v(0)]R}-1}\right] v(q)$ are put into Dyson's equation, the approximate formula obtained for the magnetization at all temperatures is

$$R = \tfrac{1}{2} - \frac{1}{N} \sum_{q} \Bigg[\tanh \frac{\beta}{2}[h+v(0)R] \div \exp \Big\{ \beta \times$$

$$\Big[\{h+v(0)R] - \{\frac{v(q)}{2} - \sum_{q'} n(q')v(q')\} \tanh \frac{\beta}{2}[h+v(0)R] - \sum_{q'} n(q')v(q-q') \tanh \tfrac{3}{2}[h+v(0)R]$$

$$+ \Big\{\bar{n} - \frac{1}{e^{\beta[h+v(0)R]}+1}\Big\} v(q) \tanh \frac{\beta}{2}[h+v(0)R] \Big] \Big\} - 1 \Bigg] \qquad \text{(V3)}$$

At low temperatures this equation reduces to equation V1 and at β_c, to equation V2.

Another check on the approximation formula is obtained by calculating the high temperature susceptibility from equation IV6. The result is

$$\lim_{\substack{\beta \to 0 \\ h \to 0}} \chi = \frac{\beta}{4} + \frac{\beta^2 v(0)}{16} + O(\beta^3 \bar{v}^2) + \ldots \qquad \text{(V4)}$$

in agreement with the known high temperature result.

B. Experimental Results

A number of ferromagnetic insulators have been discovered in recent years which provide opportunity for comparing experimental results with the predictions of statistical theories for the Heisenberg model ferromagnet. Some of these are $CrCr_3$ (Tsubokawara 1960), EuO (Mathias et al.1961), $GdCl_3$ (Wolf et al. 1962), EuS (Moruzzi and Teaney 1963) and $Cu(NH_4)_2\ Cl_4.2H_2O$ and $CuK_2Cl_4.2H_2O$ (Miedema et al. 1963). However, of these, only the copper salts measured by Miedema would be suitable for comparison with the theoretical results of this thesis, since they are the only ones with spin ½.

The dominant magnetic interactions in these copper salts are isotropic exchange interactions, and the structure of these salts, which crystallize in the tetragonal system, is closely approximated by a body-centred cubic lattice (Wood and Dalton, to be published). Each copper ion has eight nearest-neighbors (n.n.'s) at a distance of 6.6Å, and six next nearest neighbors (n.n.n.'s) at a distance of 7.45Å. Since the ratio of these distances is about 1.13, there is a strong possibility of exchange interaction between next nearest neighbor copper ions. By using the expansions of Dalton and Wood (1965) for a body centred cubic lattice in which both n.n. and n.n.n. interactions are included, Dalton and Wood (1966) estimate the ratio of the n.n.n. exchange integral to the n.n. exchange integral to be about .25 from the critical properties of the salts. Hence, the experimental behaviour of these salts is more likely to be described by the high Z or long range potential expansion of this thesis than would be the behaviour of salts with just nearest neighbor interactions. Thus, these copper salts offer a good

opportunity for comparing the theoretical results of this thesis with experiment.

Dalton and Wood (to be published) attempt to fit the magnetization curve for $CuK_2.Cl_4.2H_2O$ with spin wave theory at low temperatures with n.n.n. interactions included. Their theoretical curve falls within the experimental error of the points up to $\frac{T_c}{2}$, but for $T > \frac{T_c}{2}$ it does not approach 0 nearly as sharply as the experimental curve. In the next section an attempt is made to fit the magnetization curve of $CuK_2.Cl_4.2H_2O$ for the whole range 0 to T_c by using a long range potential in both the approximate formula given in the previous section and RPA.

C. Calculation of Approximate Curve and RPA Curve for Magnetization with Long Range Potential; Comparison with Experiment

In this section, the theoretical magnetization curves are calculated for both the approximate formula of the last section and RPA with long range potentials. The results are compared with the experimental points for the magnetization of $CuK_2.Cl_4.2H_2O$ obtained by Miedema (1963) in zero field. The RPA curve is calculated first since the calculation can be done self-consistently. Then this expression is used in the more complicated approximate formula as a first iteration. It is seen that the difference between the result of this first iteration and the RPA point is negligible.

The RPA expression for the magnetization in zero field is, from Zubarev (1960),

$$R = \tfrac{1}{2} - \frac{1}{N} \sum_{q}' \frac{2R}{e^{\beta[v(0)-v(q)]R} - 1} \qquad (V5)$$

for spin ½. The potential v(q) is treated with an approximation which is valid for long range potentials. The potential v(r) is shown in (1) of figure 16 with r_o its range, and v(q) is shown in (2) of figure 16 with q_o its range. The expression for q_o is, from Chapter III, $q_o = 2\left(\frac{4\pi\rho}{3Z}\right)^{\frac{1}{3}}$. The difference v(0)-v(q) appearing in equation V5 is the solid line shown in (3) of figure 16.

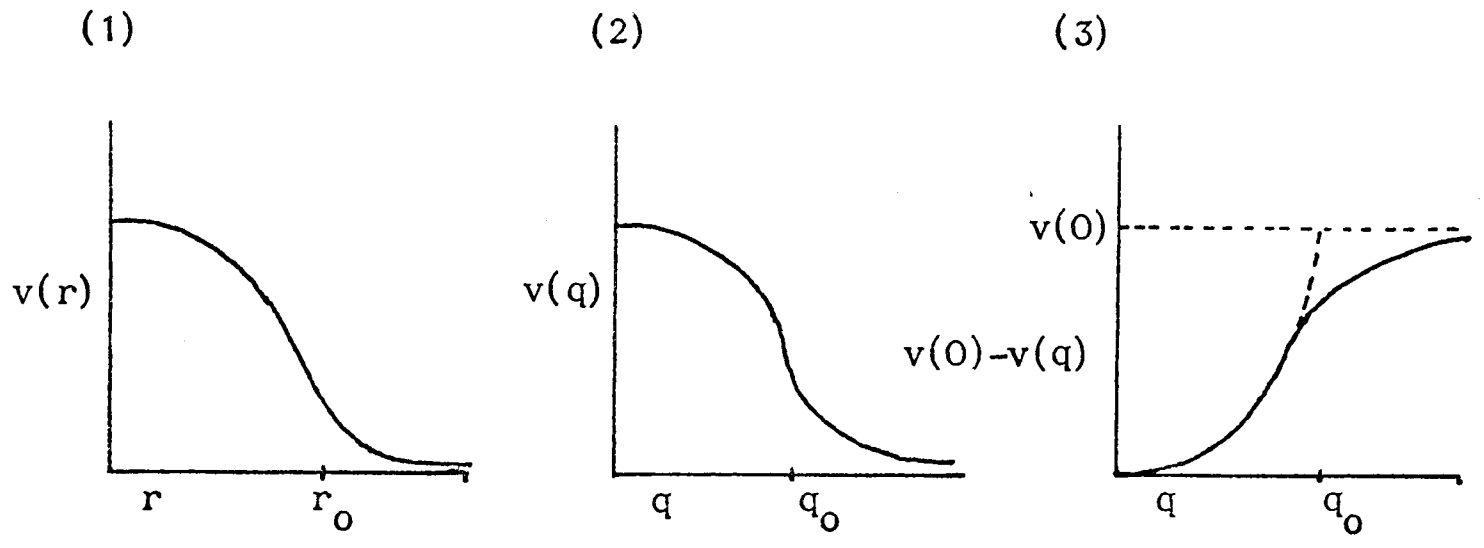


Figure 16

For high Z or a long range potential, q_o is pushed close to the origin, and the curve v(0)-v(q) may be approximated by a quadratic for $q \leq q_o$ and a constant for $q > q_o$. The quadratic curve for v(0)-v(q) must equal v(0) for $q = q_o$. Thus in this approximation

$$v(0) - v(q) = \begin{cases} \frac{v(0)}{4}\left(\frac{Z}{4/3\pi\rho}\right)^{2/3} q^2 & q \leq q_o \\ v(0) & q > q_o \end{cases} . \qquad (V6)$$

This expression is then substituted into equation V5. The summation over q in that equation is divided into the sum of terms with $q \leq q_o$ and the sum of terms for $q > q$.

$$R=\tfrac{1}{2} - \frac{1}{N} \sum_{q\leq q_o} \frac{2R}{e^{\beta\left[\frac{v(0)}{4}\left(\frac{Z}{4/3\pi\rho}\right)^{2/3} q^2\right]R} - 1} - \frac{1}{N} \sum_{q>q_o} \frac{2R}{e^{\beta\, v(0)R} - 1} \cdot \qquad \text{(V7)}$$

The terms for $q>q_o$ are independent of q, and from Chapter III it is known that there are $N\left(1 - \frac{16}{9\pi Z}\right)$ of these terms. Thus

$$\frac{1}{N} \sum_{q>q_o} \frac{2R}{e^{\beta\, v(0)R} - 1} = \frac{2R\left[1 - \frac{16}{9\pi Z}\right]}{e^{\beta\, v(0)R} - 1} \cdot \qquad \text{(V8)}$$

The summation with $q\leq q_o$ is approximated by an integral as follows.

$$\frac{1}{N} \sum_{q\leq q_o} \frac{1}{e^{\beta[\frac{v(0)}{4}\left(\frac{Z}{\frac{4}{3}\pi\rho}\right)^{2/3} q^2]R} - 1} \simeq \frac{V}{N} \frac{2R}{(2\pi)^3} \int_o^{2\left(\frac{\frac{4}{3}\pi\rho}{Z}\right)^{\frac{1}{3}}} \frac{q^2\, dq}{e^{\beta[\frac{v(0)}{4}\left(\frac{Z}{\frac{4}{3}\pi\rho}\right)^{2/3} q^2]R} - 1} = \frac{16\, R}{3\pi\, [\beta v(0)R]^{3/2}\, Z} \int_o^{\beta v(0)R} \frac{x^{\frac{1}{2}}\, dx}{e^x - 1} \qquad \text{(V9)}$$

with the change of variables $x = \frac{\beta\, v(0)R}{4}\left(\frac{Z}{4/3\pi\rho}\right)^{2/3} q^2$.

The v(0) appearing in both equations V8 and V9 may be expressed in terms of β_c through the equation for the Curie point. For RPA, this equation is (Tahir-Kheli and ter Haar 1963)

$$\beta_c = \frac{4F(-1)}{v(0)} \qquad \text{(V10)}$$

where

$$F(-1) = \frac{1}{N} \sum_q \frac{v(0)}{v(0)-v(q)} \cdot$$

The expression $v(0)-v(q)$ is approximated by equation V6 and the sum treated as above. The integral may be done immediately and the result is

$$F(-1) = 1 + \frac{32}{9\pi Z} . \qquad \text{(V11)}$$

Combining equations V7, V8, V9 and V10, yields

$$R=\tfrac{1}{2} - \frac{16R}{3\pi\left[4F(-1)\frac{\beta}{\beta_c} R\right]^{3/2} Z} \int_0^{4F(-1)\frac{\beta}{\beta_c}R} \frac{\chi^{\frac{1}{2}}dx}{e^x-1} - \frac{2R\left[1-\frac{16}{9\pi Z}\right]}{e^{4F(-1)\frac{\beta}{\beta_c}R}-1} \qquad \text{(V12)}$$

This equation can be solved self-consistently by assuming a value for the variable $Y=4F(-1)\frac{\beta}{\beta_c} R$, performing the integration, solving the equation for R, and then determining $\frac{\beta}{\beta_c}$ from the assumed value of Y and the calculated value for R. The Y values are chosen from combinations of $\frac{\beta}{\beta_c}$ and R which are close to the expected values to expedite the calculation, and the method of evaluation of the integral using tables for the incomplete gamma function is given in Appendix C.

The results of the calculation for Z=8 are given in figure 17. The choice of Z=8 should represent $CuK_2.Cl_4.2H_2O$, although if n.n.n. interactions have an exchange integral ¼ the size of the n.n. exchange integral, then Z would be $\tilde{=}$ 9, since there are 6 n.n.n.'s. However, the calculation is insensitive to changes in Z of this small a magnitude. The calculation is also done for Z=80, and the resulting curve coincides with the molecular field curve given in figure 17. In figure 17, the experimental points for $CuK_2.Cl_4.2H_2O$, T_c= .88K, (Miedema 1963) are given by dots surrounded by boxes indicating the experimental errors.

It is seen that the RPA curve for Z=8 fits within the experimental error of the points up to $\frac{T}{T_c} \tilde{=} .6$, but that it falls below the the points as the temperature increases towards T_c.

The approximate formula obtained in this thesis is given in equation V3. The field is now set equal to zero. At low temperatures, this equation reduces to equation V1 and shows the same $T^{3/2}$ behaviour as RPA. Only when the tanh factors of the approximate formula differ significantly from 1 would the two expressions give different results. This temperature is about $\frac{T_c}{4}$. For temperatures at wnich the tanh factors differ significantly from 1, it is not possible to treat the approximate formula as a function of two variables and to solve it self-consistently as is done for the RPA expression. Hence, it is necessary to use some iteration process. Since the RPA expression is similar to this expression, it is used in the first iteration by putting the RPA expressions for n(q') into equation V3.

The same approximation expression for v(q) given in equation V6 is used in all the expressions appearing in this calculation. The term $\sum_{q'} n(q')v(q-q')$ appearing in the exponential of equation V3 is approximated by

$$\sum_{q'} n(q')v(q-q') \simeq \sum_{\substack{q' \\ |q-q'|<q_o}} n(q') \left[v(0)-(q^2+q'^2-q.q') \left\{ \frac{v(0)}{4} \left(\frac{Z}{\frac{4}{3}\pi\rho} \right)^{2/3} \right\} \right]$$

$$\simeq \sum_{q'<q_o} n(q') \left[v(0)-(q^2+q'^2) \left\{ \frac{v(0)}{4} \left(\frac{Z}{4/3\pi\rho} \right)^{2/3} \right\} \right] \qquad \text{(V13)}$$

since it is expected that for a long range potential, small q will be most important and hence the sum over q' will cause the $q.q'$ terms to give nearly canceling contributions.

The sum over q in equation V3 is divided into sums for $q \leq q_o$ and $q > q_o$, and the lower sum is converted into an integral. It is noted that at temperatures for which the tanh functions differ from 1 there are q independent terms in the exponent unlike the case of RPA. Some of these q independent terms are constants and others are of the form $\sum_{q'} n(q')v(q')$. This latter term may be calculated in the same manner as the previous RPA calculation is done except that the q'^2 term coming from $v(q')$ leads to incomplete gamma functions of a higher order. When all the terms in the exponential of equation V3 are calculated and a pair of values of R and $\frac{\beta}{\beta_c}$ from the RPA curve inserted, it is seen that the integral coming from the summation for $q \leq q_o$ has a gap and is of the form

$$\int_o^a \frac{q^2\, dq}{e^{b+c\, q^2} - 1}, \quad \text{with } b \text{ a small constant.}$$

It follows that

$$\int_o^a \frac{q^2\, dq}{e^{b+c\, q^2} - 1} = \frac{1}{2c^{3/2}} \int_o^{a^2 c} \frac{x^{\frac{1}{2}}\, dx}{e^{b+x} - 1} \tag{V14}$$

under the change of variables $x = c\, q^2$. The method of evaluating the last integral is given in Appendix D.

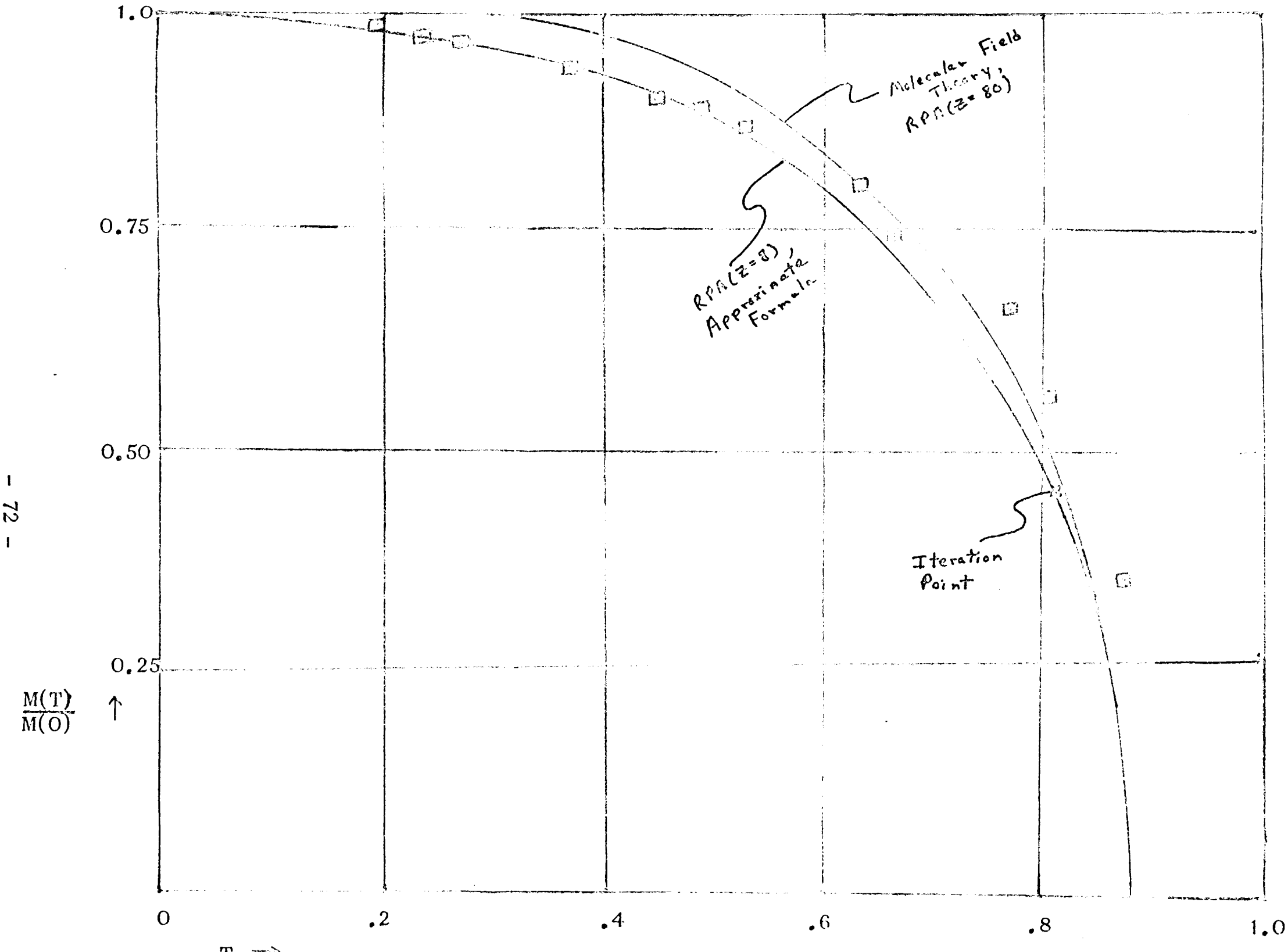
The contribution to the magnetization coming from the terms in the sum for $q > q_o$ is of the form

$$\frac{\left(1 - \frac{16}{9\pi Z}\right) \tanh\left(\frac{\beta}{2} v(0)R\right)}{e^{\beta\eta} - 1}$$

where η is a function of the q independent parts of the exponential in equation V3.

One iteration is performed for the approximate formula with the pair of values of R and $\frac{\beta}{\beta_c}$ chosen from the RPA curve in the region where that curve is significantly below the experimental points. The values chosen are $R = .233$, $\frac{T}{T_c} = .917$. Z is taken as 8 again. The calculation then gives some indication of how the approximate formula compares with RPA. The new value of R obtained for the same $\frac{T}{T_c}$ from this first iteration is $R = .234$. This point is shown in figure 17 by the cross on the RPA ($Z=8$) curve. The change in the value of R from this first iteration is much smaller than the experimental errors on the experimental points and thus is negligible. In the approximate formula, the appearance of the gap in the integral tends to make the spin wave deviation term smaller, and the molecular field theory $v(0)$ tends to make the exponential term larger than in the RPA result. It is seen that in this calculation, these effects almost cancel each other. As noted before, the magnetization expressions from RPA and the approximate formula also give the same results at low temperature $\left(0 \lesssim \frac{T}{T_c} \lesssim .4\right)$ where the $\tanh \frac{\beta}{2}[h+v(0)R]$ functions in the approximate formula are approximately 1. Thus, these results indicate that RPA and the approximate formula give similar results for the magnetization throughout the entire temperature range, $0 \lesssim T \lesssim T_c$.

Thus, the RPA (Z=8) curve in figure 17 may be taken to represent the approximate formula result also. The calculation of this one point is long, and the next iteration would be even longer since then the integrals in the exponential involving n(q') would have a gap themselves. However, the derivative of the approximate magnetization expression with respect to the R value used to start the iteration is found not to diverge, and thus no peculiar behaviour would be expected in a second iteration.



COMPARISON OF THEORETICAL MAGNETIZATION CURVES WITH EXPERIMENTAL POINTS OF $CuK_2Cl_4 \cdot 2H_2O$

FIGURE 17

CONCLUSION

In this thesis, a thermodynamic perturbation expansion for the ideal Heisenberg ferromagnet has been developed. A modified Wick's theorem proved for spin ½ and finite temperatures allows the terms in this expansion to be expressed by Feynmann like diagrams involving propagators and interactions with extra correction dotted lines between the propagators reflecting the effects of spin statistics. These diagrams are then classified according to the $\frac{1}{Z}$ order of the irreducible self-energies appearing. As Keffer (to be published) notes, direct perturbation approaches for spin systems have suffered in the past from the lack of a well-defined parameter of smallness. It is seen that in this thesis the appearance in the expansion of the parameter of smallness, $\frac{1}{Z}$, is precisely defined.

At low temperatures, the graphs generated by the irreducible self-energy of order 1 give molecular field theory, including the graphs from order $\frac{1}{Z}$ yields spin wave theory, and including the graphs of order $\frac{1}{Z^2}$ gives Dyson's results in Born approximation. The magnetization expressions from these different orders of graphs have a Curie point

because the graphs giving molecular field theory are renormalized to include in the internal loop all the graphs coming later in the expansion. Thus, these expressions have a numerator behaving as R for small R just as the denominator does. Including all graphs generated by the irreducible self-energies through order $\frac{1}{Z^2}$ yields the Curie point of molecular field theory.

The expressions for the magnetization at low temperatures and at the Curie point are used as a guide in approximating the $\frac{1}{Z^2}$ contributions to $\langle S_z \rangle$ at all temperatures, and the resulting expression for the magnetization is compared with the experimental magnetization curve for a copper salt with spin ½ and next nearest neighbor interactions, which is approximated by the long range potential or high Z treatment in this thesis. It is seen that the theoretical curve fits the experimental points at low temperatures but falls below them as the Curie point is approached.

The approximate curve is also compared with the RPA curve. The difference between these curves is negligible. However, the approximate expression has one advantage over RPA. Although experiments are not able to distinguish between a T^3 and a T^4 term in the magnetization expression at low temperatures, the approximate expression does predict a T^4 correction term to spin wave theory in agreement with Dyson while RPA predicts a T^3 correction.

APPENDIX A

CALCULATION OF G^o, MOLECULAR FIELD THEORY

In section A of Chapter II, all the g^o's are replaced by G^o's where the G^o's are the functions obtained from the summation of all graphs of the form of those in figure A1. The lines of these graphs are still g^o's.

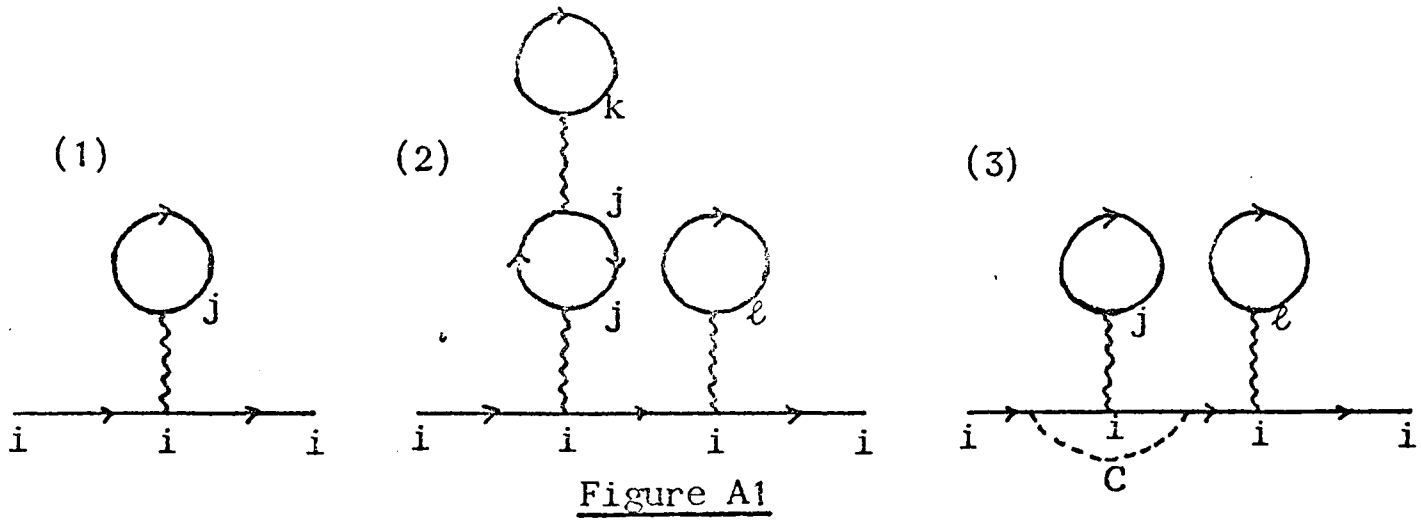


Figure A1

The difficulty of summing all the correction dotted line graphs is avoided by noting that all the graphs in this case come from the longitudinal term in H_1. The spin operators in this term appear in equal-index, equal-time pairs. Thus, if just this term of H_1 is considered, the P operators in the perturbation theory of Chapter I may be replaced by the T operator without any corrective ξ factors. The ξ factors are unnecessary because any permutation of operators to obtain the correct chronological order always involves the permutation of a pair of operators yielding a factor $(-1)^{2n} = +1$, as is obtained under the P operator. Wick's theorem for fermious may be applied directly to the T product averages appearing, and all the results of Chapter I are obtained with T replacing P and without the ξ factors. Hence, the correction dotted line graphs which accounted for the effects of the ξ

functions no longer appear. The Green's function is defined for the moment with a T instead of a P and designated $G_T(i,j)$. All the lines of the graphs may again be identified with g_T^o's.

It is possible to sum all the graphs of the form of (1) and (2) in figure A1 by making the loop in the irreducible self-energy of (1) a full G_T function and applying Dyson's equation. The fully renormalized loop is

$$G_T(j,j) = - < T \left\{ \tilde{S}_j^+(\tau_j) \tilde{S}_j^- (\tau_j) \right\} > = + \bar{n}_j = + \bar{n} \qquad (A1)$$

since $\bar{n}_j$ is independent of j. Since the loop is made a full G function, if graphs other than the graphs giving molecular field theory are included later, these graphs are automatically put into the loop and the loop remains $\bar{n}$. The summation over j may be done freely and the interaction term becomes $\sum_{\substack{j \\ j \neq i}} v_{ij} = v(0)$. The sign of the graph (1) in figure A1 is minus, and it carries a factor of $\frac{1}{2}$ because it is first order in H_1.

It is noted that because of the delta functions on the site indices of the g^o's, there are no additional internal summations over the site indices. It is also noted that because of the convolution form of the time dependence of the graphs, the internal integrations may be removed by Fourier analysis. Hence Dyson's "diagrammatic" equation may be made an algebraic equation.

The g_T^o's are given by

$$g_T^o(i,j) = e^{-[h+v(0)](\tau_i-\tau_j)} \begin{cases} -\left(1 + e^{-\beta[h+\frac{v(0)}{2}]}\right)^{-1} \delta r_i r_j & \tau_i > \tau_j \\ \left(1 + e^{\beta[h+\frac{v(0)}{2}]}\right)^{-1} \delta r_i r_j & \tau_i < \tau_j \end{cases} . \qquad (A1)$$

As a function of $\tau_i - \tau_j = \tau$, $g_T^o(i,j)$ is antiperiodic with period β and may be Fourier analyzed according to the formulas

$$G_T(\tau) = \frac{1}{\beta} \sum_n e^{-i\omega_n \tau} G_T(\omega_n) \qquad G_T(\omega_n) = \tfrac{1}{2} \int_{-\beta}^{\beta} e^{i\omega_n \tau} G_T(\tau)\, d\tau \qquad (A2)$$

where $\omega_n = \frac{(2n+1)\pi}{\beta}$ since $G_T(\tau)$ is antiperiodic. A simple calculation gives

$$g_T^o(\omega_n) = \frac{1}{i\,\omega_n - h - \frac{v(0)}{2}} . \qquad (A3)$$

If the Fourier analysis is used in Dyson's equation, the equation becomes

$$G_T^o(i,i,\omega_n) = g_T^o(i,i,\omega_n) + g_T^o(i,i,\omega_n) \sum (i,i,\omega_n)\, G_T^o(i,i,\omega_n)$$

$$= \frac{1}{g_T^o(i,i,\omega_n)^{-1} - \Sigma\,(i,i,\omega_n)} . \qquad (A4)$$

The expression for the Fourier component of the fully renormalized graph (1) of figure A1 is $- g_T^o(i,i,\omega_n) \frac{\bar{n}\, v(0)}{2} G_T^o(i,i,\omega_n)$. There is another graph appearing exactly like this graph except that the indices on the

interaction are interchanged. The two graphs correspond to graphs (1) and (3) in figure 1a. Their contributions are exactly the same and together they yield

$$\sum = - \bar{n}\, v(0) \tag{A5}$$

and

$$G_T^o(i,i,\omega_n) = \frac{1}{i\,\omega_n - h - \frac{v(0)}{2} + v(0)\,\bar{n}} = \frac{1}{i\,\omega_n - h - v(0)\,R} \,. \tag{A6}$$

It is now possible to calculate $G^o(i,i,\tau)$.

$$G_T^o(i,i,\tau) = \frac{1}{\beta} \sum_{\omega_n} \frac{e^{-i\,\omega_n \tau}}{i\,\omega_n - h - v(0)\,R} \,. \tag{A7}$$

From the method of Luttinger and Ward (1960), the sum over the ω_n may be replaced by a contour integration with respect to Z by using the function $\pm\beta \left[e^{\pm\beta Z} + 1 \right]^{-1}$ which has poles at the points $Z = \frac{(2n+1)\pi i}{\beta}$. The function is chosen to make the integrand converge for large Z. Thus

$$G_T^o(i,i,\tau) = \frac{1}{\beta} \sum_{\omega_n} \frac{e^{-i\,\omega_n \tau}}{i\,\omega_n - h - v(0)R} = \pm \frac{1}{2\pi i} \oint \frac{e^{-Z\tau}\, dZ}{\left(Z - h - v(0)R\right)\left(e^{\pm\beta Z} + 1\right)} \,. \tag{A8}$$

The result is

$$G_T^o(i,j,\tau) = + e^{-[h+v(0)R]\tau} \begin{cases} -\left(1 + e^{-\beta[h+v(0)R]}\right)^{-1} \delta r_i r_j & \tau>0 \\ \left(1 + e^{+\beta[h+v(0)R]}\right)^{-1} \delta r_i r_j & \tau\leq 0 \end{cases} . \qquad (A9)$$

Thus

$$R = \tfrac{1}{2} - \bar{n} = \tfrac{1}{2} - G_T^o(i,i,\tau=0^-) = \tfrac{1}{2} - \frac{1}{1+e^{-\beta[h+v(0)R]}} = \tfrac{1}{2} \tanh \frac{\beta}{2} [h+v(0)R] \qquad (A10)$$

which is the result of molecular field theory.

When the transverse part of H_1 is included, the Green's functions of Chapter I are the ones which must be used. These Green's functions have the P chronological operator and are periodic. To apply Dyson's equation the internal Green's functions must have the same periodicity as the Green's function being calculated. If the $G_T^o(i,j)$ calculated in this appendix is put into the internal lines of the higher order graphs of Chapter II, its periodic version must be used. Thus, the $G^o(i,j)$ to be used is the same as $G_T^o(i,j)$ given in equation A9 except that a minus sign appears in front of the expression for $\tau\leq 0$ also. The Fourier analysis of $G^o(i,j)$ involves a sum over ω_n such that $\omega_n = \frac{2\,n\,\pi}{\beta}$ since $G^o(i,j)$ is periodic. It is seen that the Fourier component giving the correct result is

$$G^o(i,i,\omega_n) = \frac{\tanh \frac{\beta}{2} [h+v(0)R]}{i\,\omega_n - h - v(0)\,R} \qquad (A11)$$

since

$$G^{o}(i,i,\tau) = \frac{1}{\beta} \sum_{\omega_n} \frac{e^{i\omega_n \tau} \tanh \frac{\beta}{2}[h+v(0)R]}{i\omega_n - h - v(0)R} \quad .$$

$$= \pm \frac{\tanh \frac{\beta}{2}[h+v(0)R]}{2\pi i} \oint \frac{e^{-Z\tau} \, dZ}{(Z-h-v(0)R)\left[e^{\pm\beta Z} - 1\right]} \quad . \qquad \text{(A12)}$$

where $\pm\beta \left(e^{\pm\beta Z}-1\right)^{-1}$ is chosen since it has poles at $Z = \frac{2n\pi i}{\beta}$. The result is exactly that of equation A9 except for a minus sign for $\tau \lesssim 0$ and is given in equation II1. This $G^{o}(i,i,\tau)$ is the function which would be obtained if the graphs of figure A1 were summed directly.

APPENDIX B

SUMMATION OF ORDER $\frac{1}{Z}$ GRAPHS

In tnis appendix, the contributions to G(i,j) from all the graphs generated by the irreducible self-energy of order $\frac{1}{Z}$ are summed using Dyson's equation. The sum includes all graphs of the form of graph (3) figure 9.

These graphs involve internal summations over indices as well as integrations over times. Introducing the Fourier analysis of the Green's function with respect to the difference of its time variables eliminates the integrations over the times as is seen in Appendix A. The spacial dependence of Green's function G(i,j) is of the form $(r_i - r_j)$ as is the spacial dependence of the exchange integral v_{ij}. Thus these functions may be Fourier transformed by the following formulas.

$$G(r_i - r_j) = \frac{1}{N} \sum_q G(q)\, e^{iq.(r_i - r_j)} \qquad v_{ij} = \frac{1}{N} \sum_q v(q)\, e^{iq.(r_i - r_j)} . \qquad (B1)$$

When these expressions are inserted into the graphs considered in this case, the internal summations over indices vanish because of the convolution form of the graphs. Dyson's equation for the ω_n and q components of G becomes algebraic.

$$G(q,\omega_n) = G^o(q,\omega_n) + G^o(q,\omega_n) \sum (q,\omega_n)\, G(q,\omega_n)$$

with $$\sum (q,\omega_n) = \frac{-v(q)}{2} \quad \text{and} \quad G^o(q,\omega_n) = \frac{\tanh \frac{\beta}{2} [h + v(0)R]}{i\,\omega_n - h - v(0)R} . \qquad (B2)$$

These equations yield

$$G(q,\omega_n) = \frac{\tanh \frac{\beta}{2}\left[h+v(0)R\right]}{i\,\omega_n - h - v(0)R + \frac{v(q)}{2}\tanh\frac{\beta}{2}\left[h+v(0)R\right]} \tag{B3}$$

The $G(i,j)$ is obtained by summing over the q's and ω_n's.

$$G(i,j) = \frac{1}{N}\sum_{q}\frac{1}{\beta}\sum_{\omega_n} G(q,\omega_n)\, e^{iq\cdot(r_i-r_j)}\, e^{-i\omega_n(\tau_i-\tau_j)} . \tag{B4}$$

The summation over the ω_n's may be performed by converting the summation into a contour integration exactly as is done in Appendix A for the case of n even. The result is

$$G(i,j) = -\frac{1}{N}\sum_{q} e^{iq(r_i-r_j)} e^{-\left\{h+v(0)R - \frac{v(q)}{2}\tanh\frac{\beta}{2}\left[h+v(0)R\right]\right\}(\tau_i-\tau_j)}$$

$$\times \tanh\frac{\beta}{2}\left[h+v(0)R\right]\begin{cases}\left[e^{-\beta\left\{h+v(0)R-\frac{v(q)}{2}\tanh\frac{\beta}{2}\left[h+v(0)R\right]\right\}}-1\right]^{-1} & \tau_i>\tau_j \\ \left[e^{+\beta\left\{h+v(0)R-\frac{v(q)}{2}\tanh\frac{\beta}{2}\left[h+v(0)R\right]\right\}}-1\right]^{-1} & \tau_i<\tau_j\end{cases} \tag{B5}$$

The expression for R obtained by including all graphs through order $\frac{1}{Z}$ is

$$R = \tfrac{1}{2} - \bar{n} = \tfrac{1}{2} + G(i,i,\tau=0^-) = \tfrac{1}{2} - \sum_{q} \frac{\tanh\frac{\beta}{2}\left[h+v(0)R\right]}{e^{\beta\left\{h+v(0)R-\frac{v(q)}{2}\tanh\frac{\beta}{2}\left[h+v(0)\right]\right\}}-1} \tag{B6}$$

APPENDIX C

CALCULATION OF INTEGRAL IN RPA CALCULATION

The integral appearing in equation V12 is

$$\int_0^{4F(-1)\frac{\beta}{\beta_c} R} \frac{x'^{\frac{1}{2}}\, dx'}{e^{x'} - 1} = \int_0^{Y} \frac{x'^{\frac{1}{2}}\, dx'}{e^{x'} - 1} \qquad (C1)$$

where Y designates the chosen value for $4F(-1)\frac{\beta}{\beta_c}$. From expanding the denominator, equation C1 becomes

$$\int_0^{Y} \frac{x'^{\frac{1}{2}}\, dx'}{e^{x'} - 1} = \sum_{n=1}^{\infty} \int_0^{Y} x'^{\frac{1}{2}}\, e^{-nx'}\, dx' = \sum_{n=1}^{\infty} \frac{1}{n^{3/2}} \int_0^{nY} x^{\frac{1}{2}}\, e^{-x}\, dx. \qquad (C2)$$

The integral in the last expression of equation C2 is an incomplete gamma function. These functions are tabulated (Pearson 1922). Also, the sum $\sum_{n=1}^{\infty} \frac{1}{n^{3/2}}$ and the integral for the range 0 to ∞ are known.

$$\xi(3/2) = \sum_{n=1}^{\infty} \frac{1}{n^{3/2}} = 2.62$$

and

$$\Gamma(3/2) = \int_0^{\infty} x^{\frac{1}{2}}\, e^{-x}\, dx = .886 \qquad (C3)$$

from tables for the zeta and complete ganna functions respectively (Jahnke, Emde and Lösch 1960). Since for $Y \geq 1.1$ $\left(\frac{T}{T_c} \leq .9,\ R \geq \frac{1}{4}\right)$ the values of the incomplete gamma function in the last expression of equation C2 differ in the third place from the values of the complete gamma function only for n less than 7, the expression in equation C2 is calculated in the following manner.

With the use of the tables for the incomplete gamma function, the expression $\sum_{n=1}^{\alpha} \int_0^{nY} x^{\frac{1}{2}} e^{-x}\, dx$ is calculated where α is the highest integer for which this incomplete gamma function with the given Y value differs from the complete gamma function in the third place. Also

$$\sum_{n=1}^{\alpha} \frac{1}{n^{3/2}} \int_0^{\infty} x^{\frac{1}{2}} e^{-x}\, dx \quad \text{and} \quad \sum_{n=1}^{\infty} \frac{1}{n^{3/2}} \int_0^{\infty} x^{\frac{1}{2}} e^{-x}\, dx \quad \text{are}$$

calculated using equations C3. Then the expression for the right side of equation C2 is given by

$$\sum_{n=1}^{\infty} \frac{1}{n^{3/2}} \int_0^{nY} x^{\frac{1}{2}} e^{-x}\, dx \simeq \sum_{n=1}^{\infty} \frac{1}{n^{3/2}} \int_0^{\infty} x^{\frac{1}{2}} e^{-x}\, dx -$$

$$\left[\sum_{n=1}^{\alpha} \frac{1}{n^{3/2}} \int_0^{\infty} x^{\frac{1}{2}} e^{-x}\, dx - \sum_{n=1}^{\alpha} \int_0^{nY} x^{\frac{1}{2}} e^{-x}\, dx \right] . \quad \text{(C4)}$$

Thus, the integral appearing in equation V11 is evaluated. For $\frac{T}{T_c} > .9$, $R < \frac{1}{4}$, α rapidly becomes larger and the calculation more tedious.

APPENDIX D

EVALUATION OF THE INTEGRAL IN APPROXIMATE FORMULA CALCULATION

The integral in equation V14 is

$$\int_0^{a^2c} \frac{x'^{1/2}\,dx'}{e^{b+x'}-1} \quad .$$

It is evaluated by the same general approach used in Appendix C. The integrand may be expanded as follows.

$$\int_0^{a^2c} \frac{x'^{1/2}\,dx'}{e^{b+x'}-1} = \sum_{n=1}^{\infty} e^{-nb} \int_0^{a^2c} x'^{1/2}\, e^{-nx'}\, dx' = \sum_{n=1}^{\infty} \frac{e^{-nb}}{n^{3/2}} \int_0^{na^2c} x^{1/2}\, e^{-x}\, dx. \qquad (D1)$$

The integral on the right is again an incomplete gamma function, and the evaluation can be done in the same way as in Appendix C if the sum $\sum_{n=1}^{\infty} \frac{e^{-nb}}{n^{3/2}}$ is known.

This sum is evaluated for small b by using the expansion given by London (1964) for

$$F_\sigma(b) = \frac{1}{\Gamma(\sigma)} \int_0^{\infty} \frac{x^{\sigma-1}}{e^{x+b}-1}\, dx = \sum_{n=1}^{\infty} \frac{e^{-nb}}{n^{\sigma}} \quad . \qquad (D2)$$

In particular

$$F_{3/2}(b) = \sum_{n=1}^{\infty} \frac{e^{-nb}}{n^{3/2}} = -3.545\, b^{1/2} + 2.612 + 1.460b - 0.104b^2 + .00425b^3 - \ldots \qquad (D3)$$

Thus from the known values of $\sum_{n=1}^{\infty} \frac{e^{-nb}}{n^{3/2}}$ and the complete gamma function

$\int_0^\infty e^{-x} x^{\frac{1}{2}} dx$, the right hand side of equation D1 is calculated from the formula

$$\sum_{n=1}^{\infty} \frac{e^{-nb}}{n^{3/2}} \int_0^{na^2c} e^{-x} x^{\frac{1}{2}} dx \cong \sum_{n=1}^{\infty} \frac{e^{-nb}}{n^{3/2}} \int_0^{\infty} x^{\frac{1}{2}} e^{-x} dx -$$

$$\left[\sum_{n=1}^{\alpha} \frac{e^{-nb}}{n^{3/2}} \int_0^{\infty} x^{\frac{1}{2}} e^{-x} dx - \sum_{n=1}^{\alpha} \int_0^{na^2c} x^{\frac{1}{2}} e^{-x} dx \right] \qquad \text{(D4)}$$

where α is determined in the manner of Appendix C, and the Pearson (1922) tables are used for the values of the incomplete gamma function. For the point chosen for the start of the interation in Chapter V, $b = .0653$; so the convergence of the series in equation D3 is rapid.

APPENDIX E

LIFETIMES OF EXCITATIONS AT LOW TEMPERATURES

In this appendix it is shown that at low temperatures, the order $\frac{1}{Z^3}$ graphs with their internal lines renormalized with graphs through order $\frac{1}{Z^2}$ lead to the same expression for the damping coefficient of spin wave excitations found by Tahir-Kheli and ter Haar (1963), who use the equations of motion of the advanced and retarded Green's functions with Dyson's ideal Hamiltonian.

The graphs from the expansion of Chapter II with irreducible self-energies of order $\frac{1}{Z^3}$ are of the form of those shown in figure E1.

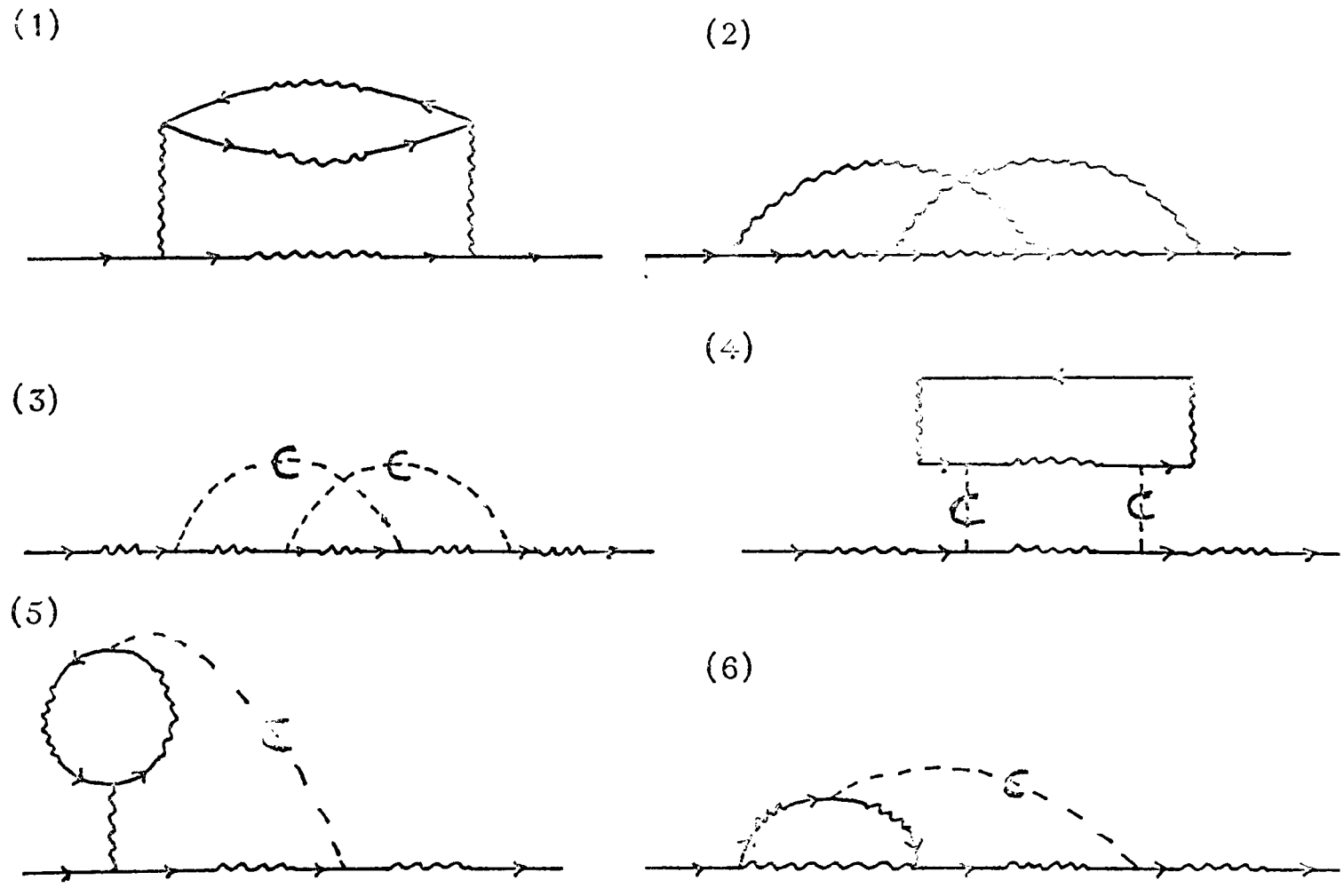


Figure E1

All these graphs involving correction dotted lines are treated exactly as graphs (4) and (5) of figure 9 are treated at low temperatures in Chapter III. The result is that graphs of the type of (3) and (4) of figure E1 together yield graphs (3) and (4) of figure E2, graph (5) of figure E1 yields graphs (5) and (6) of figure E2, and graphs (6) of figure E1 yields graphs (7) and (8) of figure E2. Graphs (1) and (2) of figure E1 go over directly to graphs (1) and (2) of figure E2.

The ω_n and q dependencies of the graphs are given in figure E2. The bold lines represent the sum of all the graphs generated by the irreducible self-energies through order $\frac{1}{Z^2}$. The q and ω_n components of these lines are, from Chapter III,

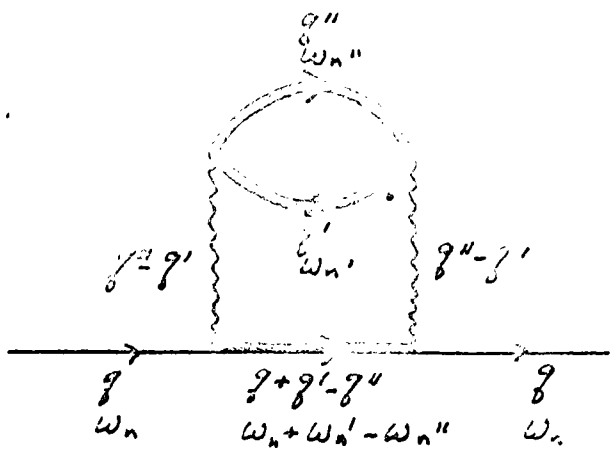
$$G(q,\omega_n) = \frac{1}{i\,\omega_n - \varepsilon_1(q)} \tag{E1}$$

where

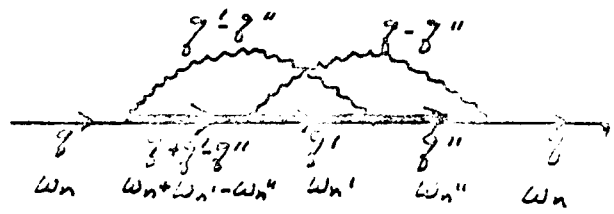
$$\varepsilon_1(q) = \tfrac{1}{2}\,[v(0)-v(q)] + \sum_{q'} n(q')\,[v(q')+v(q) - v(q'-q) - v(0)].$$

The signs and factors of the graphs of figure E2 are determined by the signs and factors of the graphs of figure E1 from which they come. Graphs (1) and (2) carry factors of +1 since the factor of ¼ from the interactions is canceled by the factor of 4 coming from the interchange of the indices on the ends of each longitudinal interaction. Graphs (3) and (4) also have a +1 factor since the +4 from the two dotted lines is canceled by the factor ¼ from the two interactions. Graphs (5),(6),(7) and (8) all have (-1) factors from the product of the -2 from the one dotted line, the 2 from the interchange of indices on the ends of the

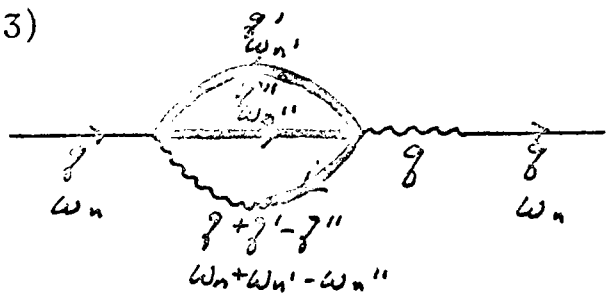
(1)



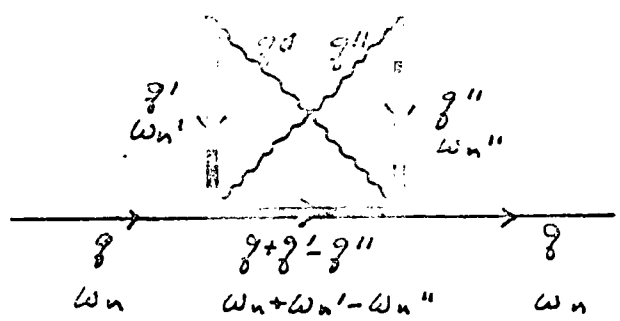
(2)



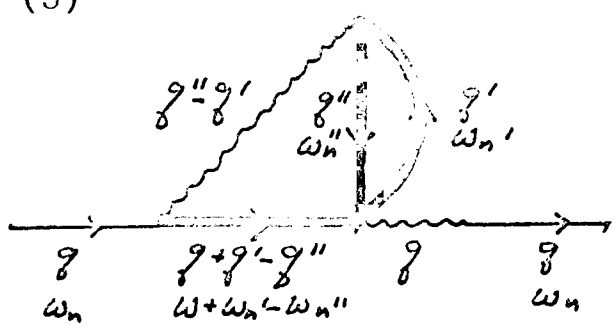
(3)



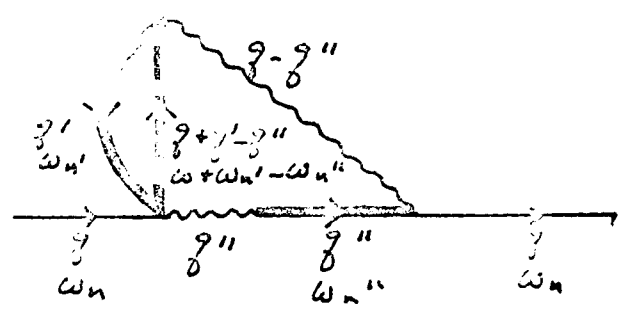
(4)



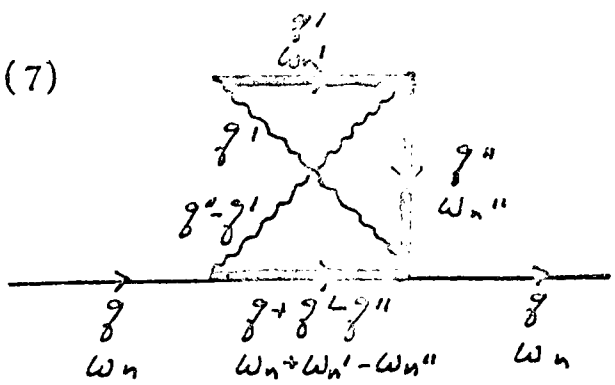
(5)



(6)



(7)



(8)

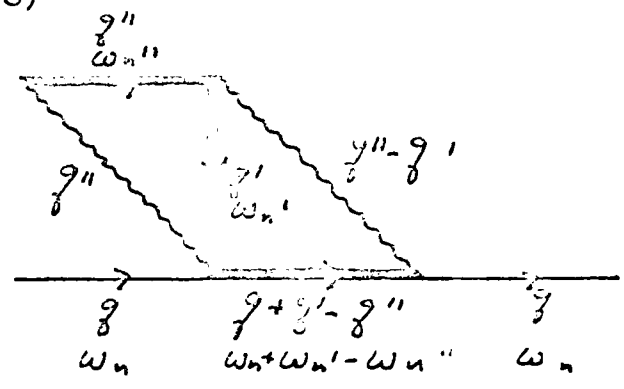


Figure E2

longitudinal interaction, and the ¼ from the interaction terms.

Each of the irreducible self-energies of figure E2 is now calculated for use in Dyson's equation. The calculation is done below for only the irreducible self-energy of graph (1), figure E2. All the other calculations are exactly the same except for the interaction terms appearing. The irreducible self-energy of graph (1), $\Sigma^{(1)}(q,\omega_n)$ is given by the following equation.

$$\Sigma^{(1)}(q,\omega_n) = \sum_{\substack{\omega_{n'} \\ \omega_{n''}}} \int \frac{dq'\, dq'' \left[v(q''-q')\right]^2}{\left[i\,\omega_{n''}-\varepsilon_1(q'')\right]\left[i\,\omega_{n'}-\varepsilon_1(q')\right]\left[i(\omega_n+\omega_{n'}-\omega_{n''})-\varepsilon_1(q+q'-q'')\right]} \qquad \text{(E2)}$$

The sum over the ω_n's is performed by converting to a contour integral in the method of Appendix A, $\sum_{\omega_n} \rightarrow \pm \frac{\beta}{2\pi i} \oint \frac{dZ}{e^{\pm Z}-1}$. Either of the factors $\frac{1}{e^{\pm Z}-1}$ can be chosen since the integral converges for large Z for both of them because each $i\omega_n,(Z)$, appears in two factors in the denominator of equation E2. The factor $\frac{1}{e^{+Z}-1}$ is chosen here. Thus

$$\sum^{(1)}(q,\omega_n) = \sum_{\omega_{n''}} \int \frac{dq'dq'' \left[v(q''-q')\right]^2 \left[n(q')-n(q+q'-q'')\right]}{\left[i\omega_{n''}-\varepsilon_1(q'')\right]\left[i\omega_n+\varepsilon_1(q')-i\omega_{n''}-\varepsilon_1(q+q'-q'')\right]}$$

$$= \int \frac{dq'dq'' \left[v(q''-q')\right]^2 \left[n(q')-n(q+q'-q'')\right]\left[n(q'') \quad e^{-\frac{1}{\beta[\varepsilon_1(q')-\varepsilon_1(q+q'-q'')]}} -1\right]}{i\,\omega_n + \varepsilon_1(q') - \varepsilon_1(q'') - \varepsilon_1(q+q'-q'')} \qquad \text{(E3)}$$

where n(q) is taken to be

$$n(q) = \frac{1}{e^{\beta\varepsilon_1(q)} - 1}$$

in a Born approximation.

The following identities are true.

$$n(q')-n(q+q'-q'') = \left[e^{\beta[\varepsilon_1(q+q'-q'')-\varepsilon_1(q')]} -1\right]\left[1+n(q')\right] n(q-q'-q'') \qquad \text{(E4)}$$

and

$$n(q'') - \frac{1}{e^{\beta[\varepsilon_1(q')-\varepsilon_1(q+q'-q'')]} - 1} = \frac{e^{-\beta[\varepsilon_1(q')-\varepsilon_1(q'')-\varepsilon_1(q+q'-q'')]} -1}{e^{\beta[\varepsilon_1(q+q'-q'') - \varepsilon_1(q')]} - 1} n(q'').$$

Putting these expressions into equation E3 yields

$$\sum^{(1)}(q,\omega_n) = \int \frac{dq'dq'' \left[v(q''-q')\right]^2 \left[e^{\beta[-\varepsilon_1(q')+\varepsilon_1(q'')+\varepsilon_1(q+q'-q'')} -1\right]\left[1+n(q')\right]n(q+q'-q'') \times n(q'')}{i\omega_n + \varepsilon_1(q') - \varepsilon_1(q'') - \varepsilon_1(q+q'-q'')} \qquad \text{(E5)}$$

This expression may be compared with the corresponding expression of Langer (1962) for fermions. It may be simplified further to give

$$\sum^{(1)}(q,\omega_n) = \int \frac{dq'dq''\left[v(q''-q')\right]^2\left\{n(q')\left[1+n(q'')+n(q+q'-q'')\right]-n(q'')n(q+q'-q'')\right\}}{i\,\omega_n+\varepsilon_1(q')-\varepsilon_1(q'')-\varepsilon_1(q+q'-q'')} \tag{E6}$$

Each of the other irreducible self-energies of figure E2 leads an expression differing from equation E6 only in the interaction term. These interaction terms may be taken directly from the graphs themselves. The sum of all these interaction terms may be put into a symmetric form by interchanging the q'' line of the graph and the $q+q'-q''$ line, taking the new interactions into the sum, and dividing the sum by two. The sum of these interactions is

$$D(q,q',q'') = \tfrac{1}{2}\left[v(q')+v(q)-v(q''-q')-v(q-q'')\right]\times$$

$$\left[v(q'')+v(q+q'-q'')-v(q''-q')-v(q-q'')\right]. \tag{E7}$$

The expression for the sum of all the irreducible self-energies of figure E2 is thus

$$\sum^{(T)}(q,\omega_n) = \int \frac{dq'dq''\,D(q,q',q'')\left\{n(q')\left[1+n(q'')+n(q+q'-q'')\right]-n(q'')n(q+q'-q'')\right\}}{i\,\omega_n+\varepsilon_1(q')-\varepsilon_1(q'')-\varepsilon_1(q+q'-q'')}. \tag{E8}$$

If this self-energy along with the self-energies leading to $\varepsilon_1(q)$ is put into Dyson's equation for $G(\omega_n,q)$, the result is

$$G(\omega_n, q) = \frac{1}{i\,\omega_n - \varepsilon_1(q) - \varepsilon_2(q,\omega_n)} \quad . \tag{E9}$$

where $\varepsilon_2(q,\omega_2) = \Sigma^T(q,\omega_n)$. To obtain the excitation spectrum and the damping coefficient associated with the spectral intensity, it is necessary to make an analytic continuation of the function $G(\omega_n)$ into the upper and lower half planes (Abrikosov, Gorkov and Dzyaloshinski 1963). In the upper half plane $G^+(\omega) = G^R(\omega)$ and in the lowerhalf plane $G^-(\omega) = G^A(\omega)$ where $G^R(\omega)$ and $G^A(\omega)$ are respectively the advanced and retarded Green's functions. Thus equation E9 becomes

$$G^{\pm}(\omega_{\pm}, q) = \frac{1}{\omega_{\pm} - \varepsilon_1(q) - \varepsilon_2(q,\omega_{\pm})} \tag{E10}$$

where $\omega_+ = \omega + i\varepsilon$ and $\omega_- = \omega - i\varepsilon$.

The expression for $\varepsilon_2(q,\omega_{\pm})$ may be written in the following form.

$$\varepsilon_2(q,\omega_{\pm}) = R(q,\omega_{\pm}) \mp i\gamma(q,\omega_{\pm}) \tag{E11}$$

where

$$R(q,\omega) = P \int \frac{dq'dq''\ A(q,q',q'')}{\omega + \varepsilon_1(q') - \varepsilon_1(q'') - \varepsilon_1(q+q'-q'')} \quad ,$$

$$\gamma(q,\omega) = \pi \int dq'dq''\ A(q,q',q'')\ \delta\left[\omega + \varepsilon_1(q') - \varepsilon_1(q'') - \varepsilon_1(q+q'-q'')\right] \quad ,$$

and

$$A(q,q',q'') = D(q,q',q'') \left\{ n(q') \left[1+n(q'')+n(q+q'-q'') \right] - n(q'')n(q+q'-q'') \right\} .$$

Thus

$$G^{\mp}(\omega_{\pm},q) = \frac{1}{\omega_{\pm} - \varepsilon_1(q) - R(q,\omega_{\pm}) \mp i\gamma(q,\omega_{\pm})} \qquad \text{(E12)}$$

which is the expression Tahir-Kheli and ter Haar (1963) find.

From this point, the development proceeds as in Tahir-Kheli and ter Haar. The spectral intensity is defined by

$$< S_q^-(t') \; S_q^+(t) > = \int_{-\infty}^{\infty} f(E) \, dE \, e^{-i E(t-t')} . \qquad \text{(E13)}$$

It satisfies the equation

$$i \, F(E) \, (e^{\beta E}-1) = G^-(q) - G^+(q) . \qquad \text{(E14)}$$

Combining equations E10, E11 and E14 yields

$$F(E) \, (e^{\beta E}-1) = \frac{1}{\left[E-\varepsilon_1(q) - R(q,E) \right]^2 + \gamma(q,E)^2} . \qquad \text{(E15)}$$

Tahir-Kheli and ter Haar (1963) show that $R(q)$ and $\gamma(q)$ are small quantities which vanish as T tends to zero. The right side of equation E15 is strongly peaked at an energy $\bar{\varepsilon}(q)$ given by

$$\bar{\varepsilon}(q) - \varepsilon_1(q) - R[\bar{\varepsilon}(q)] = 0$$

since $\gamma(q)$ is of as smaller order of magnitude than $R(q)$ (Tahir-Kheli and ter Haar 1963). It is seen that $R[\bar{\varepsilon}(q)]$ gives an energy shift and that $\gamma(q)$ is a damping coefficient. Tahir-Kheli and ter Haar (1963) indicate a proof which shows that the damping coefficient is related to the lifetime τ through the equation

$$\gamma(q)\,\tau(q) = \hbar \tag{E16}$$

and that $\gamma(q)$ first contributes to the temperature expansion for the magnetization in the $T^{9/2}$ term.

It is noted that all the low temperature results of this appendix and also those of Chapter III may be obtained immediately from a diagrammatic expansion like that of Chapter I using Dyson's ideal Hamiltonian for $S=\frac{1}{2}$.

$$H_{ideal} = \left(+ h + \frac{v(0)}{2}\right) \sum_i b_i^+ b_i - \tfrac{1}{2} \sum_{i \neq j} v_{ij}\, b_i^+ b_j$$

$$+ \tfrac{1}{2} \sum_{i \neq j} v_{ij} \left[b_i^+ b_j^+ b_j b_j - b_i^+ b_i b_j^+ b_j \right] \tag{E17}$$

where $S_i^- = b_i - b_i^+ b_i$, $S_i^+ = b_i^+$ and $S_i^z = b_i^+ b_i - \tfrac{1}{2}$.

The b operators obey boson commutation relations and the expansion is made just as for bosons. The linked graphs obtained are of the form of (1) and (2) of figure 1a, (1) of figure 1b and (3) and (4) of figure 11 in first order and of the form of the graphs of figure E2 in second order.

Acknowledgements

My sincere thanks to:

Dr. R.B. Stinchcombe, my supervisor, for his instruction and assistance during this work and also for his enthusiasm, encouragement, and advice.

My colleagues, Drs. Pettick and Marquard, and Messrs Moore, Stenholm and Das for interesting discussions on all subjects.

The Rhodes Trustees, for the award of a Scholarship.

The Department of Theoretical Physics and New College for their hospitality during my three years at Oxford.

Jutta, for special assistance during the latter stages of the preparation of the manuscript.

Bibliography

Abrikosov, A.A., L.P. Gorkov and I.E. Dzyaloshinski (1963) Methods of Quantum Field Theory in Statistical Physics, translated by R.A. Silverman, Prentice-Hall Inc., Englewood Cliffs, New Jersey.

Berlin, T.H. and M. Kac (1952), Phys. Rev. 86, 821.
Bloch, F. (1930), Z. Physik. 61, 206.
Bloch, F. (1932), Z. Physik. 74, 295.
Bloch, M. (1962), Phys. Rev. Letters 9, 286.
Bogolyubov, N.N. and S.V. Tyablikov (1959), Dokl. Akad. Nauk. S.S.S.R. 126, 59 [translation: Soviet Phys.-Doklady 4, 589 (1959)]
Brout, R. (1960), Phys. Rev. 118, 1009.
Brout, R. (1961), Phys. Rev. 122, 469.

Callen, H.B. (1963), Phys. Rev. 130, 890.
Carleton, H.R., R. Brout and R. Stinchcombe (1965), J. of Applied Physics, 36, 1138.
Copeland, J.A. and H.A. Gersch (1966), Phys. Rev. 143, 236.

Dyson, F.J. (1956), Phys. Rev. 102, 1217.
Dyson, F.J. (1956), Phys. Rev. 102, 1230.

Englert, F. (1960), Phys. Rev. Letters 5, 102.

Gossard, A.C., U. Jaccarino and J.P. Remeika (1961), Phys. Rev. Letters 7, 122.

Horwitz, G. and H.B. Callen (1961), Phys. Rev. 124, 1757.

Jahnke, Emde and Lösch (1960), Tables of Higher Functions, 6th ed., McGraw-Hill Book Company Inc., New York.

Keffer, F. (to be published) Handbuck der Physik 18.

Landau, L.D. and E.M. Lifshitz, (1958), Statistical Physics, translated by E. Peierls and R.F. Peierls, Addison-Wesley Publishing Co., Inc., Reading, Mass.
Langer, J.S. (1962), Phys. Rev. 127, 5.
London, F. (1964), Superfluids, Vol.2, Dover Publications, Inc., New York.
Low, G.G. (1963), Proc. Phys. Soc. (London), 82, 992.
Luttinger, J.M. and J.C. Ward (1960), Phys. Rev. 118, 1417.

Mathias, B.T., R.M. Bozorth and J.H. van Vleck (1961), Phys. Rev. Letters 7, 1960.
Matsubara, T. (1955), Prog. Theor. Phys. 14, 351.
Miedema, A.R., H. van Kempen and W.J. Huiskamp (1963), Physica 29, 1266.
Mills, R.L., R.P. Kennan and J. Korringa (1960), Physica 26, 5204.
Moruzzi, V.L. and D.T. Teaney (1963), Solid State Comm. 1, 127.

Pearson, K. ed.(1922), Tables of the Incomplete Γ-Function, Dept. of Applied Statistics, University College, University of London, published by His Majesty's Stationery Office for the Department of Scientific and Industrial Research, London.

Schweber, Silvan, S. (1961), An Introduction to Relativistic Quantum Field Theory, Harper and Row, New York.
Stinchcombe, R.B., G. Horwitz, F. Englert and R. Brout (1963), Phys. Rev. 130, 155.

Tahir-Kheli, R.A. and D. ter Haar (1962), Phys. Rev. 127, 88.
Tahir-Kheli, R.A. and D. ter Haar (1962), Phys. Rev. 127, 95.
Tsubokawara, I. (1960), J. Phys. Soc. Japan 15, 1664.

Wang, Y., S. Strikman and H.B. Callen, (1965) (to be published).
Weiss, P. (1937), Ext. Actes VII. Congr. Intern. Froid 1, 508.
Wolf, W.P., M.J.M. Leask, B. Mangum and A.F.G. Wyatt (1962), J. Phys. Soc. Japan 17, S487.
Wood, D.W. and N.W. Dalton (1965) (to be published).

Zubarev, D.N. (1960), Uspekhi Fiz. Nauk. 71, 71 [translation: Soviet Physics Uspekhi 3, 320 (1960)].